

We deeply thank Dr. Thompson and the anonymous referee for the valuable comments and suggestions, which help us improve the quality of the manuscript. All the comments have been addressed and the detailed responses to each comment are shown as following.

#### **1. To Editor**

(1) We found that Figure 7(b) in the previous versions of the manuscript was wrong. It was generated from an incomplete version of results. We have replotted the plot with the correct results in the revised manuscript. There is no problem with the other plots in the figure.

(2) As said in our response to the minor comment on Lines 437-440 and the original Figure 8 from the second referee, we decided to delete the original Figure 8 in the revised manuscript.

We meant to demonstrate that the model has the skill to simulate the spatial distribution of the total atmospheric IWC by showing Figure 8. However, it seems to make little sense to the purpose of this manuscript (demonstrating that the inclusion of dust effect improves the simulation of cloud ice), as there is no visible difference between the IWP from CTRL and DUST. This is because that the IWP measured by MODIS includes not only cloud ice, but also precipitable ice, such as snow and graupel. However, the inclusion of dust effect in the simulation greatly affects the amount of cloud ice, but hardly influence the amount of precipitable ice, and cloud ice accounts for less than 1/10 of the total atmospheric IWC, therefore, the increase of cloud ice cannot significantly influence the total amount of atmospheric IWC, as shown in the original Figure 8.

## 2. Response to Dr. Gregory Thompson

Scientific issues:

Computational time needed for the new treatment.

Response: As dust is produced by WRF-Chem for the new treatment of dust-ice interaction, it requires longer computational time than using standard WRF only. Generally, the speed ratio between standard WRF and WRF-Chem with the GOCART aerosol scheme is 5:3.

In our opinion, it brings improvements either by directly incorporation a dust emission into WRF, or hooking up the GOCART aerosol scheme and microphysics scheme. It is more efficient in computing dust-ice interaction with the first option. However, there are several dust emission schemes in the GOCART aerosol scheme, and more will be added. These dust emission schemes might have different performances depending on the regions. Therefore, it allows users to apply different dust emission schemes to produce dust emission for evaluating dust-ice interaction by hooking up the GOCART aerosol scheme with microphysics scheme.

Thanks very much for the information about your work, we have mentioned the extra computational time needed for the simulation (WRF-Chem with GOCART) in section 2.1, and we also discussed about the alternate possibility in the introduction in the revised manuscript.

Statistics for the performance of the model in simulating AOD and PM<sub>10</sub> concentration.

Response: The correlation coefficients for AOD is 0.46 and 0.65 for Dalanzadgad and SACOL, respectively. The statistics for the surface PM<sub>10</sub> concentrations are displayed in Table 2, but we have also put the correlation coefficient of each station in Figure 3 and 4 in the revised manuscript.

Minor comments:

Comment 1: At line#106 and similar lines mentioning the "Thompson scheme," would you please change all relevant places to "Thompson-Eidhammer scheme?" I would like to ensure proper credit to the coauthor of the WRF aerosol-aware scheme.

Response: we have replaced "aerosol-aware Thompson scheme" with "Thompson-Eidhammer scheme" in the revised manuscript.

Comment 2: Line#118: you state: "In the current version of WRF-Chem..." then mention the number of water/ice-friendly aerosols. Actually, this is not technically correct as the creation of those 2 variables does not occur within any version of WRF-Chem. Those new variables are created irrespective of WRF-Chem for correctness in the paper.

Response: We have revised the statement into "For the Thompson-Eidhammer scheme...".

Comment 3: Lines 126-128: "... can hardly represent realistic aerosol level..." is a bit too harsh.

Actually, the use of a climatological aerosol concentration is closer to observations more often than not simply because the times when aerosols are extremely high or low as compared to climatology are the rarity in the true world as it takes a major weather change to produce the more extreme values. Take for example a place in the world with consistent southerly winds and a large urban region to the south of a point in question.

When the winds are from the north, from a region of very low aerosols, then the point in question may be experiencing a large departure from climatology. Or if a significant weather front moves through a region and pushes away a majority of the aerosols, then the departure from average is more significant than the days in which the "regular weather regime" is occurring. So I am only suggesting to you that the wording here could be an exaggeration that using climo aerosols is always wrong.

Response: We have modified this part to make a fairer statement in the revised manuscript.

Comment 4: Line 205 and 223: The internals of the Thompson-Eidhammer scheme contains a wet deposition removal by precipitation. Did you disable this internal sink of aerosols when putting in your own wet removal process or is there a double-counting of aerosol removal?

Response: Yes. The GOCART aerosol scheme calculates the number concentration of aerosol every time step, it makes no sense to update it in the Thompson-Eidhammer scheme, so we turned it off while calculating the wet deposition using a new scheme.

Comment 5: Fig. 6b: I believe the units label is incorrect if the plot is supposed to show cloud ice number concentration.

Response: Revised in the updated manuscript.

Comment 6: Fig. 7: Can you offer any explanation for the very very large increase in ice number concentration showing along the southern boundary of the domain? The increase looks tremendous.

Response: During dust season, the outbreak of cold high system over northeast Asia can bring quantitative dust aerosol down to the South China Sea or even further, a typical case on March 26, 2012 is shown in Fig. R1 attached at the end of this response. In such cases, strong northwesterlies swept across the entire China, and brought large amount of dust from source areas to the south border of the domain. Besides, the water vapor mixing ratio over south China Sea can be over five times as that over north China as shown in Fig. R2. Large amount of ice nuclei transported by winds, combining with abundant water vapor, results in a significant enhancement in the formation of ice crystals over the area.

Comment 7: Line 433-434: If moist convection is too weak in the model and insufficient water vapor is not lofted high enough, then do you mean there is an \*under\* prediction of ice water path? The text says there is an over-prediction, but I do not understand this apparent contradiction.

Response: It was a mistake and should be “underestimation”, we have corrected it in the revised manuscript.

Comment 8: Fig. 11: Is the peak shown ~4km coinciding with the melting level? If so, is it a data processing issue of falsely identifying ice clouds in CALIPSO data?

Response: The melting level is slightly below 4 km for the cases in Fig. 11, it is reasonable that ice clouds are observed at 4km, but the small peak at ~2 km in the third case in Fig. 11 might be due to falsely identifying ice clouds in CALIPSO data.

Comment 9: Line 531: "...once the coagulation makes the relative humidity..." I cannot determine how the word coagulation is being used here. Can you please re-phrase this sentence?

Response: It has been revised in to “freezing of droplets” in the updated manuscript.

Comment 10: Figs. 12 and 13: Is the ice water content computed from a combination of cloud ice mixing ratio and snow? I strongly advise combining both since cloud ice species in Thompson is literally only the smallest ice crystals (generally mean sizes below 40 microns) whereas the snow is much larger (mixing ratio as well as mean size).

Response: The ice water content shown in Fig. 12 and 13 contains only cloud ice. The reason we did not use a combination of cloud ice mixing ratio and snow is that, the ice water content in CALIPSO products represents only the amount of cloud ice, as the CALIPSO instruments are more sensitive to ice clouds and liquid clouds composed of small particles or droplets, and the LIDAR signal emitted from CALIPSO attenuated rapidly in optically dense clouds (more detailed description can be seen in section 5.2.2).

Therefore, for comparison of the vertical profile of ice water content with the CALIPSO products, we only apply the mixing ratio of cloud ice.

The combination of simulated cloud ice mixing ratio and snow is compared to MODIS products in Fig. 8, but only for a spatial comparison, due to the limitation of observations.

Comment 11: Line 567: "A new microphysics scheme..." Calling this entirely a 'new' scheme is probably a stretch. The microphysics scheme is still much more than dust nucleating as ice, so a 'new treatment' for a source of dust used in the existing scheme is perhaps a more fair description.

Response: we have revised it into “a new treatment” to avoid overstate the implementation work.

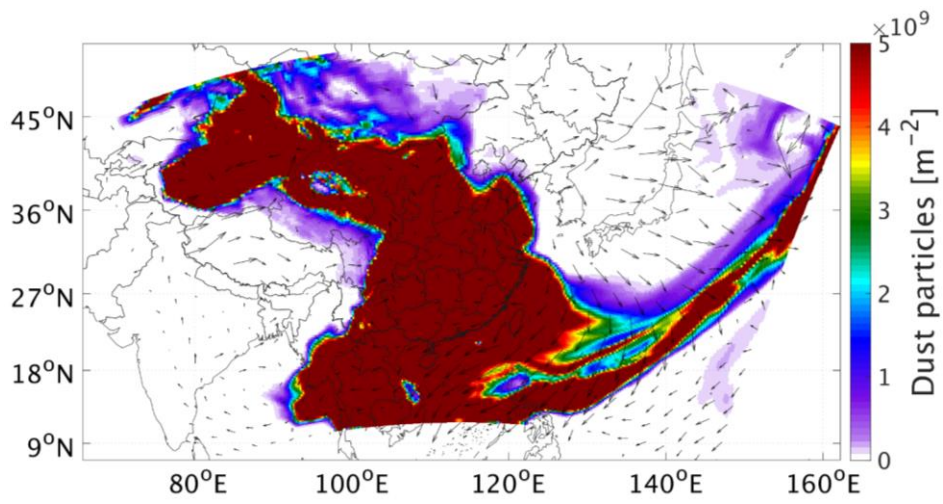


**Fig. R1:** The spatial distribution of dust particle number density over East Asia at 04 UTC, March 26, 2012.

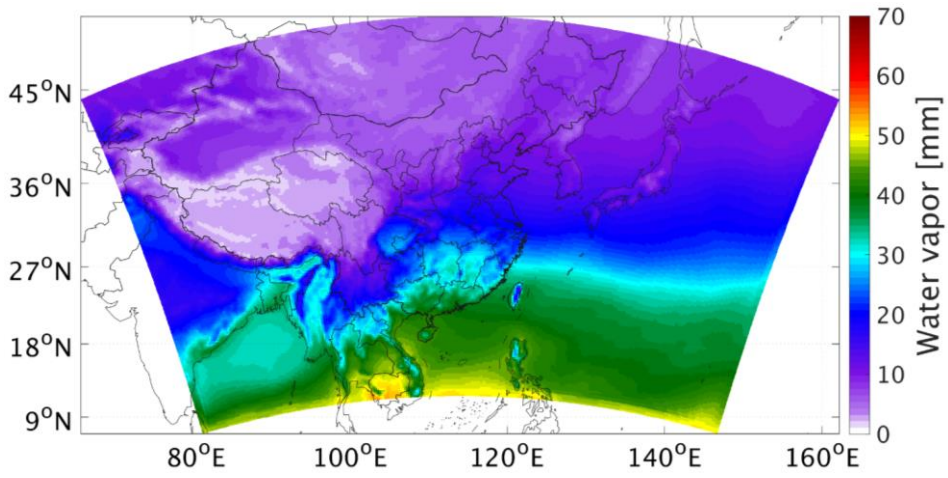


**Fig. R2:** The spatial distribution of the mean column sum of water vapor over East Asia during the simulation period.

### 3. Response to the anonymous referee #2

#### General Comments:

Comment #1: It is a bit confusing the fact that the authors sometimes write that the improvements are due to the application of the newly-implemented GOCART-Thompson microphysics scheme (e.g. line 29) and other times that the improvements are due to the consideration of dust effect (e.g. line 508). In this work, all the simulations use the newly-implemented GOCART-Thompson microphysics scheme (as written at line 252) and the dust emissions are switched on in the DUST simulation while they are switched off in the CTRL one. As a consequence, if Fig. 8, 9, 10, 11 show that DUST is better than CTRL in comparison with the observations, the reason is the inclusion of dust effect in ice nucleation (not the application of the newly-implemented GOCART-Thompson microphysics scheme, although the dust effect in ice nucleation can be considered only thanks to the GOCART-Thompson microphysics scheme). Therefore, I would correct lines 29, 506-508 (while lines 452-453 are correct). Strictly speaking, the improvements due to the application of the newly-implemented GOCART-Thompson microphysics scheme could be demonstrated only by a comparison between the standard version of WRF-Chem and the “new” version WRF-Chem + the newly-implemented GOCART-Thompson microphysics scheme.

Response: We have modified the manuscript to clarify that the improvement in the simulation of ice water content was due to the inclusion of dust effect.

Comment #2: In CTRL results, are the ice crystals only produced by homogeneous nucleation? And what about IWP and IWC in Fig. 8, 9, 10, 11? Some words should be spent also to explain CTRL results, as they also show weak signals in correspondence to the dust events (although without dust emissions).

Response: Ice crystals can be produced by both homogeneous nucleation and heterogeneous nucleation in CTRL run. We have clarified it in section 3. In both CTRL and DUST, the newly-implemented GOCART-Thompson microphysics scheme was used for condensation and immersion freezing; the deposition nucleation is determined by the parameterization of Phillips et al. (Phillips et al., 2008), and the freezing of deliquesced aerosols using the hygroscopic aerosol concentration is parameterized following Koop et al. (Koop et al., 2000), with the background aerosol concentration set to be 1/L, which means that in CTRL, the background aerosol concentration is 1/L.

Comment #3: The advantages of using the newly-implemented GOCART-Thompson microphysics scheme should be stressed more in comparison to the standard version of WRF-Chem (e.g. in the section about the implementation). For instance, besides the possibility to consider the dust effect on ice nucleation, the coupling allows to consider it during particular episodes like intensive dust events. What about simulations with other aerosol species emissions?

Response: We have added a paragraph at the end of section 2 to stress the advantage of coupling the GOCART aerosol model with the Thompson-Eidhammer microphysics scheme.

Comment #4: As dust particles come from different sources (also anthropogenic), please, specify that here dust is actually “mineral dust” (at least at lines 22 in the abstract, 37, 42, ...), although this should be clear because “natural

sources" are mentioned at the beginning of the Introduction. Please, quantify (percentage ?) how much dust contributes to the global aerosol burden at line 37.

Response: We have specified in the manuscript that only "mineral dust" was produced in the DUST simulation. The contribution of dust to the global aerosol burden has been added in Section 1.

Comment #5: Just as general comment, my thought is that CTRL simulation with no aerosol emissions at all is a rather "extreme" scenario. I would have preferred to keep more realistic aerosol emissions (including for example black carbon, organics, ...) and to reduce dust emissions (e.g. by 50%) in CTRL, instead of excluding them.

Response: Other than to evaluate performance of the newly-implemented treatment in simulating ice nucleation involving dust aerosol, we wanted to investigate the effects of dust on the regional weather system over East Asia (which was presented in part II of this paper), therefore, the CTRL run must be an "extreme" scenario without dust aerosol.

Comment #6: The authors should define more explicitly the direct, semi-direct and indirect effects of dust in the paragraph between the lines 42-48, because these effects are then commented in the next paragraph (from line 49). It would be nice also to add some lines (between 46-48) about the role of dust in ice nucleation, as it is the crucial process considered in the paper (heterogeneous nucleation, nucleation modes, thermodynamic conditions,...). Parts of lines 65-66 could be moved here.

Response: The second paragraph in Section 1 has been revised to explicitly the direct, semi-direct and indirect effects of dust.

Comment #7: It would be appropriate to develop the paragraph 93-96 by adding some information about the WRF model and the comparison between WRF and WRF-Chem (what can you do with the second one that you cannot do with only WRF? Or, why is it better to use WRF-Chem instead of WRF? In terms of aerosols and ice nucleation processes...). This addition is needed because I guess that the authors will speak about the WRF model after the requests by the first Referee.

Response: We have included the information about the comparison between WRF and WRF-Chem in Section 1: "Therefore, the aerosol-aware Thompson-Eidhammer scheme is an ideal microphysics scheme for evaluating the effect of dust in atmospheric ice nucleation processes. However, this scheme is not coupled with any aerosol model in WRF-Chem, the Weather Research and Forecast model coupled with Chemistry. When the aerosol-aware Thompson-Eidhammer microphysics scheme is activated, the model reads in pre-given climatological aerosol data derived from the output of other global climate models, which introduces large errors into the estimation of the effects of dust in microphysical processes. This problem can be solved by embedding a dust scheme into Thompson-Eidhammer scheme, or couple the microphysics scheme with WRF-Chem. Compared with WRF, WRF-Chem integrates various emission schemes and aerosol mechanisms for simulating the emission, transport, mixing, and chemical transformation of aerosols simultaneously with the meteorology (Grell et al., 2013). Therefore, WRF-Chem

is more capable of producing a realistic aerosol field by comparing the performances of different emission schemes or aerosol mechanisms.”

Comment #8: Subsection 2.3 starts saying that the modifications made by the authors are three, but then 4 sub-subsections follow. Since the sub-subsections 2.3.2 describes how the ice nucleation is treated by the aerosol-aware Thompson scheme (and, if I am correct, there are no indications about modifications by the authors in 2.3.2) I would suggest to reorder the structure of the current section 2.

I think it would be clearer for the reader first to get to know the ice nucleation scheme (what is written in 2.2 and 2.3.3), and then to focus on the implementation work done by the authors. Thus, it would be better to split section 2 in two parts: Section 2: Model description, with 2.1 and 2.2 (= 2.2 + 2.3.3) Section 3: Implementation of GOCART-Thompson microphysics scheme, with 3.1 (=2.3.1), 3.2 (=2.3.3), and 3.3 (=2.3.4). Moreover, it would be appropriate to say explicitly what the authors mean with “GOCART- Thompson microphysics scheme” (at the beginning of the new section 3?).

Response: We have re-ordered the subsections as suggested. The meaning of GOCART-Thompson microphysics scheme has been added at the beginning of section 3.

Comment #9: It is not clear to me if the DeMott2015 scheme is already available in the aerosol-aware Thompson microphysics scheme or not. At line 121 the authors say that condensation and immersion freezing is parameterized by DeMott2010, while at line 192 they say that they apply DeMott2015. Please, clarify this.

Moreover, why do the authors well explain the schemes by DeMott and they do not describe the scheme by Phillips et al. 2008? Maybe they could add just few lines also for the latter scheme.

Response: The default scheme for condensation and immersion freezing in Thompson-Eidhammer scheme is DeMott2010 scheme. Although the DeMott2015 scheme has been implemented in the code of the Thompson-Eidhammer scheme, it cannot be used without modifying the code. We modified the code to call the DeMott2015 scheme in Thompson-Eidhammer scheme for the condensation and immersion freezing in our simulations.

We explained the DeMott schemes in detail because we made some modifications in this part of code and would conduct sensitivity experiments on the parameter  $c_f$  in the DeMott2015 scheme. To avoid making it too redundant, we did not explain the other schemes in the manuscript. We think that the readers could refer to the references for the other schemes.

Comment #9: Just to be sure, the simulated data plotted in Fig. 3, 4, 5 belong to the test run DUST (not to CTRL), is it correct? Please, specify it.

Response: Yes. We have specified it in the beginning of subsection 5.1.

Comment #10: In Fig. 5, the authors focus their attention on the circled area with dust sources. However, there is an evident difference between the simulated and the observed AOD values over India and South China. Could they explain why?



Response: The high AOD values over India and South China are attributed to anthropogenic aerosols. As we did not include emissions other than dust in the simulations, the high values over these regions could not be produced. Only those high values due to dust aerosol in the circled area were produced. We have clarified it in section 5.1.3.

Minor comments:

Technical Comments / Suggestions:

Lines 30-33: I would stop the first sentence after “scheme” at line 31, and I would join “Results suggest that...” with the last sentence. Here, I would only mention that the ice nucleation scheme is not much sensitive to the calibration factor without specifying the numbers (I think this information is too specific for the Abstract).

Response: Revised as suggested.

Lines 61-62: Please, introduce here the abbreviations CCN and IN and use them in the rest of the text.

Response: Revised.

Line 69: Add reference after “WRF-Chem” or rephrase the sentence, otherwise it seems that GOCART has been implemented by the authors.

Response: The reference has been added.

Lines 74-77: I would change the sentence to: “IN 2014, the aerosol-aware Thompson microphysics scheme, which takes into account the aerosols serving as CLOUD CONDENSATION NUCLEI AND ice nuclei, has been implemented into WRF, enabling the model to explicitly predict the number concentration for cloud droplets AND ICE CRYSTALS (Thompson and Eidhammer, 2014).” Would it be correct?

Response: Revised as suggested.

Lines 82-85: This paragraph should be developed and made clearer.

The first point is the implementation, the second point is the validation plus investigation. Thus, it would be better to split the sentence in two parts and to mention also the validation of the model.

Please, explain what is the meaning of “online simulations” or write differently (probably it is better to rephrase the sentence as the expression “online simulations” does not appear again in the text, so it is not important to introduce it here).

Moreover, I would specify “THE GOCART aerosol model” at line 82: “we AIM to fully couple the aerosol-aware Thompson microphysics scheme with THE GOCART aerosol model in ...”.

I think it would be clearer since only the GOCART aerosol mode has been mentioned until this point and only later, at line 95, the reader will discover that GOCART is one of three schemes.

Response: The paragraph has been rewritten.

We have replaced “online simulation” with “WRF-Chem integrates various emission schemes and aerosol mechanisms for simulating the emission, transport, mixing, and chemical transformation of aerosols simultaneously with the meteorology”.

Revised.

Line 101: Is there a reference about the implementation of GOCART into WRF-Chem to add here?

Response: The reference has been added.

Lines 104-105: It is not clear the correspondence between the emission schemes and the list of references.

Please, write: \Shao's dust emission scheme (REF) is one of the three dust emission schemes in the GOCART aerosol model. THE OTHER TWO SCHEMES ARE DEFINED BY REF-1 AND REF-2”.

Otherwise, simply write: “Shao's dust emission scheme (REF) is one of the dust emission schemes in the GOCART aerosol model” without saying “three”.

Response: Revised as suggested.

Lines 113-116: As far as I understood, the aerosol-aware version of the Thompson scheme is the evolution of the Thompson scheme. Please, add the reference for the Thompson scheme at line 113 and for the aerosol-aware Thompson scheme at line 116.

It would be better to write “... and therefore it explicitly predicts the number concentrations of cloud condensation nuclei and ice nuclei as well as the number concentration of cloud droplets and ice crystals ”. Or, did I misunderstand the meaning?

Response: Revised as suggested.

Lines 149-152: Nicer to read: “... can be approximated through the mean effective radius (rdust, UNIT) and density (pdust, UNIT) OF DUST PARTICLES for that size bin:” deleting line 152.

Please, specify always the UNIT, e.g.: (A, UNIT). Also at line 159.

Response: Revised as suggested. The units have been added.

Line 153: More correct should be “DUST number concentration (N, #/kg) for ...” instead of “The aerosol number concentration N ...”. Also at line 156.

Response: Revised.

Line 169: According to the reference DeMott et al. 2010, nice;Tk in equation (4) is actually nIN;Tk defined as number concentration of IN (instead of ice crystal number concentration). I would follow the notation and the variable descriptions of the reference.

The same is valid for equation (5).

Then, the authors could add that  $n_{IN} = n_{ice}$  as generally IN are not enough to deplete supersaturation (if this were the case, the more efficient IN would nucleate first and  $n_{ice}$  would be less than  $n_{IN}$ ).

Response: Revised as suggested.

Lines 173, 177: Again, according to DeMott et al., I think it should be "... or low concentration of IN compared ..." and "... or higher concentrations of IN based ...", instead of "ice crystals".

Response: Revised.

Lines 174, 181: If the authors refer to Fig. S1 of DeMott2010, the relationship is between IN number concentrations and aerosol particle number concentrations (not ice crystals).

Similarly at line 181.

Response: Revised.

Lines 201-209: These two paragraphs describe how to implement the GOCART-Thompson scheme, but they are badly written (the explanations are not clear and some of them are redundant).

The authors should check this sub-subsection and rewrite it more clearly.

Response: We have rewritten the subsection and deleted the redundant content.

Lines 229-230: Delete "for the following simulation". I mean: "The mass mixing ratio for dust aerosol in a particular size bin  $n$  is then updated FOR the next time step ( $t + 1$ ):"

It would be more correct to use labels for the time in equation (8), e.g.:  $C_{t+1} = C_t - w_{etscavt}$ .

Response: Revised.

Line 233: The wet removal of dust is proportional to the concentration of what? Dust number concentration? Please, specify it.

Is there a reference to add for the wet deposition scheme in the GOCART aerosol model?

Response: The wet removal of dust is proportional to the concentration of the number concentration of dust particles.

We have clarified it in the revised manuscript.

The reference has been added.

Line 245: Information about the model time step could be added.

Response: The time step for the simulation (120s) has been added.

Line 256: It is better to write here that no other aerosol emissions are considered besides dust (what written at line 358), so the reader knows this when the analysis starts.

Does it mean that ice nucleation in CTRL occurs only via homogeneous nucleation? Please, write it.

Response: We have clarified in section 4 that there were no other aerosol emissions being considered in the simulations.

Ice crystals are produced by both homogeneous nucleation and heterogeneous nucleation in CTRL and DUST run. We have clarified it in section 3. In both CTRL and DUST, the newly-implemented GOCART-Thompson microphysics scheme was used for condensation and immersion freezing; the deposition nucleation is determined by the parameterization of Phillips et al. (Phillips et al., 2008), and the freezing of deliquesced aerosols using the hygroscopic aerosol concentration is parameterized following Koop et al. (Koop et al., 2000), with the background aerosol concentration set to be 1/L, which means that in CTRL, the background aerosol concentration is 1/L.

Lines 264-265: Are there some references for the washout method and the volume-averaging method?

Response: The references have been added.

Lines 274-278: This paragraph should be rearranged and PM10 should be defined. Moreover, the word “trend” is not used with its statistical meaning (the authors do not compute any trend of dust concentration, rather they check the magnitude and the behaviour of the temporal series). For this reason it would be better to avoid the use of “trend” (also in the next text) and to use, for instance, behaviour, evolution, etc.

Possibility for this paragraph: “The observations of surface concentration of particulate matter with diameter  $< 10 \mu\text{m}$  (PM10) measured at ten environmental monitoring stations were used to examine the capability of the model in reproducing dust levels at the ground surface during the simulation period. The ten stations (indicated by blue dots in Figure 1) were located in or surrounding the dust source areas in East Asia: Jinchang, Gansu Province, Yinchuan, Qinghai Province, Shizuishan, Ningxia Province, Baotou, Inner Mongolia, and Yan'an, Shaanxi Province.”

At the end the authors could add some characteristics of the measurements: hourly and which unit?

Response: Revised as suggested.

Lines 334-336: It seems to me that the third bin is more often comparable to the second one than to the fourth one, so I would mention here only “fourth and fifth”.

Please, quantify “major part” and “minor fraction”, as done for Fig. 2b (lines 340-341).

Response: Revised as suggested.

Lines 337-342: Is the number density vertically integrated? Please, specify it.

In Fig. 2, “ice-friendly aerosol” is written in the caption and “aerosol number” in the y-axis, while the text refers only to dust particles. The fact that dust particles are the only aerosols (ice-friendly aerosols) emitted comes out only later (line 358). It would be better to mention this already in the section of Model Configurations (and write “dust aerosol” in Fig. 2).

Response: The label of y-axis has been revised into “dust particle number”.

Line 348: Please, write that the time series of the simulated concentrations are extracted from the nearest grid point to the geographical coordinates of the stations. Is it correct?

Response: The information has been added.

Lines 349-352: This paragraph should be modified. I do not see that the surface PM10 concentration was overestimated at one station in Jinchang", the general tendency of the model should be considered before the individual events (the sentence in lines 353-354 could be moved here), and Fig. 3g and h should be also mentioned.

Thus, the paragraph could become: Overall, the model shows a good performance in simulating the dust cycle at THE different LOCATIONS, with EVOLUTION and magnitude of the daily mean PM10 concentration well captured at most of the stations. THE MODEL TENDS TO PRODUCE SURFACE PM10 CONCENTRATIONS LOWER THAN THOSE OBSERVED, AS NO OTHER EMISSIONS WERE CONSIDERED IN THE SIMULATIONS. HOWEVER, the dust events on MARCH 21 AND April 26 WERE overestimated BY THE MODEL at the LOCATIONS in ... " c, d, g, h, i, j.

Response: Revised as suggested.

Line 360: To compute the correlation, which data are used? Hourly measurements and which simulated concentrations? Please, specify it.

Response: The correlation was calculated from the daily mean observed surface PM<sub>10</sub> concentration and the corresponding simulated values from DUST, we have clarified it in section 5.1.1.

Lines 369-372: This paragraph should be a bit modified. It would be better to say firstly the general performance of the model (remembering that the underestimation is due to the fact that there are no other emissions apart from dust) and to point out later the overestimations in the two periods.

Remember to avoid the usage of "trend".

The temporal means of simulated and observed AOD could be added.

The same considerations are valid for the next paragraph regarding SACOL.

Response: Revised as suggested.

Lines 377: In this sub-subsection both modeled results and observations are analysed, therefore, the title could be changed from "Satellite-observational AOD" to "AOD spatial distribution".

Response: Revised as suggested.

Line 385: Is it possible to quantify (percentage?) "lower values"?

Response: AOD values over TD observed by MISR are around 50% lower than those by MODIS in both March and April.

Line 388: Actually, with a first look at the plots in Fig. 5 it does not seem that the model well reproduces the evolution from March to April because the AOD looks higher in March than in April (while the observations show the opposite, as written at line 383). I see that the motivations for such sentence are provided in the next lines but, please, make line 388 clearer (and more modest).

“trend” → “evolution”.

Response: Revised as suggested.

Lines 391-393: Add some numbers (AOD means over GD and TD?).

Response: The simulated and observation AOD mean over TD and GD have been added in subsection 6.1.3.

Lines 406-412: Add the mean values of cloud ice mixing ratio and ice crystal number concentration averaged over the domain 1 (?) and the simulated period, for DUST and CTRL.

Response: The mean values of cloud ice mixing ratio and ice crystal number concentration averaged over the domain 1 and the simulation period have been added in subsection 6.2.1.

Lines 421: Write the explanation for the strong positive bias over the southern part of the domain in Fig. 7.

Response: During dust season, the outbreak of cold high system over northeast Asia can bring quantitative dust aerosol down to the South China Sea or even further. In such cases, strong northwesterlies swept across the entire China, and brought large amount of dust, especially fine particles, from source areas to the south border of the domain. Besides, the water vapor mixing ratio over south China Sea can be over five times as that over north China. Large amount of ice nuclei transported by winds, combining with abundant water vapor, results in a significant enhancement in the formation of ice crystals over the area.

We have explained it in section 6.2.

Lines 437-440: It is still not clear to me why CTRL and DUST show almost the same ice water path.

Response: The IWP measured by MODIS shown in Figure 8 includes not only cloud ice, but also precipitable ice, such as snow and graupel. The inclusion of dust effect in the simulation greatly affects the amount of cloud ice, but hardly influence the amount of precipitable ice, and cloud ice only accounts for less than 1/10 of the total atmospheric IWC, therefore, the increase of cloud IWC induced by dust did not result in a visible difference between the IWP produced from CTRL and DUST shown in Figure 8.

We meant to demonstrate that the model had the skill to simulate the spatial distribution of the total atmospheric IWC by showing Figure 8. But we decided to delete the figure in the revised manuscript, as it makes little sense to the purpose of this manuscript (demonstrating that the inclusion of dust effect improves the simulation of cloud ice).

Lines 451: Difficult to appreciate that the ice water path over dust source regions is higher in DUST than in CTRL. Is it possible to add a temporal-spatial mean computed for this region?

Response: See the response to the above comment. The figure has been deleted in the revised manuscript.

Line 459: Please, specify if the simulated profiles refer to exactly the same time (e.g. 06 UTC, ...) of the observations or if they have been averaged (daily means?).

Response: The simulated profiles are at the same hour with the observations. We have clarified it at the beginning of subsection 6.2.2.

Lines 468-469: The sentence is not clear in my opinion. What do the authors mean with “points”?

Response: The sentence has been revised into “...the CALIPSO observations of IWC are mostly at the locations where the temperatures is lower than  $-40^{\circ}\text{C}$  and the altitude is greater than 6 km poleward to 12 km equatorward...”

Lines 478-479: As both CTRL and DUST use the newly-implemented GOCART-Thompson scheme (as written at line 252), I think this sentence is not technically correct: the higher IWC values are due to the fact that in DUST the effect of dust is considered (and not to the use of the GOCART-Thompson microphysics scheme). Is it correct? Like it is written at lines 530-531.

Response: The sentence has been corrected.

Lines 505-508: According to the same considerations written above, please, rephrase also this sentence.

Response: Corrected.

Line 520: Before analysing the single cases, please, describe the main discrepancies: peaks of DUST are always lower in altitude and in magnitude.

Response: The statement has been added in subsection 6.2.3.

Lines 545-549: Not well formulated.

Moreover, why is the calibration factor linked to the relative humidity? It is not clear to me the reasoning which leads the authors to their conclusion.

Response: The paragraph has been rewritten and moved to the end of subsection 6.3.1.

As ice nucleation occurs only in a super-saturated atmosphere with respect to water vapor, the ice nucleation process would be terminated in the GOCART-Thompson microphysics scheme when the environmental  $\text{RH}_i$  is lower than the threshold  $\text{RH}_i$ , which was set to 105% for the simulations in this study. The consistency in the simulated IWC with increasing  $c_f$  for the cases in Figure 11 indicates that in these cases, the environmental  $\text{RH}_i$  had already reached below 105% when  $c_f$  was set to 3, meaning that the water vapor available for freezing into ice crystals has been consumed up with  $c_f$  equal to 3, therefore, increasing  $c_f$  could not lead to a further increase in simulated IWC. Given the above, lowering the threshold  $\text{RH}_i$  might result in an enhancement of the simulated IWC.

Lines 551-554: No profile matches the observations, better to write for instance: “... and WAS CLOSER TO the observed profile when ...”.

“... set to 3 AND 6, ..”.

Delete the part starting with “although”: the difference between 3 and 6 is too small that I would not assert this.

Response: Revised as suggested.

Line 563: I would have said 4 or 5... Also at line 603 in the Conclusions.

Response: Revised.

Line 600: Please, add that the model generally underpredicts the IWC.

Response: Revised.

Text corrections / suggestions:

Line 20: Better "... and THE aerosol-aware ..." ?

Response: Revised.

Line 24: I would switch the order because I think that the typical season is spring, not spring 2012: "... during spring, a typical dust-intensive season, in 2012."

Response: Revised.

Line 26: "increases by" → "increase UP TO".

Response: Revised.

Line 28: "demonstrated" → "demonstrateS" (the present tense is used in the Abstract).

Response: Revised.

Lines 38-39: Repetition of the word "major", possibly find a synonym.

Response: Revised.

Line 42: "Dust in the atmospherE ALTERS ...".

Response: Revised.

Line 43: No comma after "atmosphere".

Response: Revised.

Line 45: No comma after "cloud".

Response: Revised.

Line 46: No comma after "nuclei".

Response: Revised.

Line 49: "To date, many studies ..." (with \m" in lower case).



Response: Revised.

Line 54: Better "... on dust-cloud interactionS ...".

Response: Revised.

Line 60: Better "... considering aerosol-cloud interactionS ...";

"... in regional MODELS, ...";

No comma after "schemes".

Response: Revised.

Line 62: No comma after "treated".

Response: Revised.

Lines 59-63: The sentence is too long in my opinion and not very clear in the second part.

Response: The sentence has been rewritten.

Line 75: Remove "droplet" (it is specified in the next line).

Response: Revised.

Line 80: "... climate modelS, which ...".

Response: Revised.

Line 90: "... IN section 6."

Response: Revised.

Line 94: "... and the interactionS in between ...".

Response: Revised.

Line 99: "... sulfate, MINERAL dust, ...".

Response: Revised.

Line 107: No comma after "2016".

Response: Revised.

Line 118: "... number concentrationS using ...".

Response: Revised.

Lines 118-123: The sentence is too long in my opinion, the authors could separate the liquid part from the ice part.

Write in parenthesis only the year.

Response: The sentence has been rewritten.

Line 123: "... water dropletS is ...".

Response: Revised.

Line 128: Repetition of the word "multiple", possibly find a synonym.

Response: Revised.

Line 133: Better "... aerosol-cloud interactionS ...".

Response: Revised.

Lines 138-140: Maybe not very clear: "modifications" (line 138) of what?

One possibility could be: "To investigate the real-time indirect effects of dust aerosol over East Asia, the GOCART model HAS BEEN COUPLED TO the aerosol-aware Thompson microphysics scheme. TO DO THIS, WRF-Chem version 3.8.1 HAS BEEN MODIFIED IN THREE STEPS: modification of ..." or something similar.

Response: Revised.

Line 145: "... the number concentrationS of aerosols are ...";  
"... to evaluatE ...".

Response: Revised.

Line 156: Put "n" in italic style, like at line 153.

Response: Revised.

Line 158: No comma after "study".

Response: Revised.

Lines 164-165: I would move the reference to line 164: "(DeMott et al., 2010, hereafter DeMott2010 scheme)".

Response: Revised as suggested.

Lines 166: Delete "to account for condensation and immersion freezing" it is obvious from two lines before.

Response: Revised.

Line 170: Put "a, b, c, d" in italic style.

Response: Revised.

Line 176: Similarly to before, I would write: "(DeMott et al., 2015, hereafter the DeMott2015 scheme)".

Response: Revised as suggested.

Lines 177-178: Repetition of the word "latest", possibly find a synonym.

Response: Revised.

Line 181: "DeMott2015" (with "M" in upper case).

Response: Revised.

Lines 185-187: The last sentence could be deleted, there is nothing new with respect to the sentence at lines 176-178.

Response: The sentence has been deleted.

Line 188: "The number concentration of ice crystals produced by ..." without the word "that" and the singular form for "concentration" (otherwise, later, it should be: "is" → "are" and "that" → "those").

Response: Revised.

Line 193: Add comma after the first "scheme".

Response: Revised.

Lines 210-212: Move "is calculated" before: "... at grid point (i,j,k) is calculated, I.E. the tendency of ...".

Response: Revised.

Line 222: "... the fraction of dust particle for each size bin ( $\phi$ , UNIT) can be ...".

Response: The unit has been added.

Line 226: "... the loss of dust mass due to the microphysical processes (wetscav, UNIT) for a particular size bin n is ...".

Response: The unit has been added.

Lines 236-237: In my opinion, it would be nicer to specify and describe the two experiments from the beginning, as the characteristics written in the following lines actually regard both of them and not only "A numerical experiment" as written at the start of the sentence. Therefore, I would move the lines 251-252 near to 236-237, e.g.: \TWO numerical experimentS WERE conducted to examine the performance of the newly-implemented GOCART-Thompson microphysics scheme in simulating the ice nucleation process induced by dust in the atmosphere. One

control run (CTRL) was conducted without dust and one test run (DUST) was conducted with dust, both using the GOCART-Thompson microphysics scheme.". In this case, the first sentence at line 251 should be removed.

Response: Revised as suggested.

Line 238: Where? "... dust events in 2012 OVER EAST ASIA were ...".

Response: Revised.

Line 239: Remove "for this numerical test".

Response: Revised.

Line 241: The analysis has not started yet, therefore: "further" → "the".

Response: Revised.

Line 246: "simulationS".

Response: Revised.

Lines 247-248: No comma after "km".

Response: Revised.

Line 249: Specify here (TD) and (GD), as used in Fig. 1.

Response: Revised.

Line 256: Add comma after "East Asia".

Is "Shao's dust emission" the subject? If yes, "were" → "was".

Response: Revised.

Line 262: " , the gravitational..." → " ; the gravitational...".

Response: Revised.

Lines 265-266: The sentence about CTRL could be moved at line 256, so it is in contrast to DUST. I.e.: "...used to generate dust emission in the test run DUST. As no dust emission is produced in CTRL,...".

Response: Revised as suggested.

Line 269: Write in parenthesis only the year.

Response: Revised.

Line 284: Remove the sentence with the meaning of AOD. It is not necessary. Otherwise, it would

be better to add the meanings also for the other quantities (aerosol extinction and single-scattering albedo).

Response: Revised as suggested.

Lines 294, 321: "observes" → "measures".

Response: Revised.

Line 295: "... spectral BAND centred at ...".

Response: Revised.

Line 301: Earth's changes of what? E.g.:?

Response: The sentence has been rewritten.

Line 303: "; such as deserts," can be removed, because it is said before.

Response: Revised.

Line 307: "... at 550 nm..." (remove "a").

Response: Revised.

Line 333: Please, rephrase the sentence after the comma.

Response: The sentence has been rewritten.

Line 339: Or simply: "... between the TWO time series lies in ...".

Response: Revised.

Lines 345-347: \To evaluate the performance of WRF-Chem in reproducing dust emissionS over East Asia, the simulated surface PM10 concentrationS were compared with THE observations from

THE ten environmental monitoring stations located near dust sources and downwind areas (DESCRIBED IN SUBSECTION 4.1)."

Delete "at the ten stations" at line 347.

Response: Revised as suggested.

Lines 355-357: Delete "of" after "all".

Response: Revised.

Line 378: "The spatial distribution of MONTHLY mean simulated AOD was compared with ...".

Response: Revised.

Lines 379-382: It would be nicer to explain firstly what the circled area indicates and to describe later the AOD values inside the circle, so exchange the order.

Response: Revised as suggested.

Line 386: Remove "for the observations".

Add that the similarity is stronger with MODIS.

Response: Revised.

Line 389: "... the mean OBSERVED AOD was higher in the southern part of the Taklimakan Desert than that in the northern part in March and showed an increase ...".

Response: Revised.

Line 398: Given the content of this subsection and the other sub-subsections, I would personally change the title to something like "Cloud ice over East Asia" (similarly to 5.1 Dust over East Asia).

Response: The title has been changed to "Cloud ice over East Asia".

Lines 400-405: Sentence too long and not well written. The part "as the ice nucleation process is triggered by dust particles at appropriate temperature and relative humidity," can be deleted, it is a repetition. A new sentence could then start as: "Figure 6 shows the overall comparison ...".

Response: The sentence has been rewritten.

Line 405: No new line.

Response: Revised.

Line 416: Remove "spatial pattern of the".

Response: Revised.

Line 427: "The mean simulated ice water ..." → "The simulated ice water path AVERAGED over the simulation period ...". The same at line 593.

Response: Revised.

Line 432: Remove last "in".

Response: Revised.

Line 434: No comma after "Hymalayas".

Response: Revised.

Line 439: Remove "in the simulation,".

Response: Revised.

Line 448: "overestimation" → "underestimation".

Response: Revised.

Lines 456-527: Use sometimes "IWC" (defined at line 323) instead of "ice water content".

Response: Revised.

Line 458: Make reference to Fig. 9 and Fig. 10 (not to Fig. 11 which is described in the next subsection).

Response: Revised.

Line 485: Remove "through areas with heavy dust load", it is not really so.

Response: Revised.

Line 490: It is not really "east coast"...

Response: Revised.

Line 495: "well" → "better".

Response: Revised.

Line 497: "in East China" → "from the dust sources".

Response: Revised.

Line 497: "in to" → "into".

Response: Revised.

Line 514: Fig. 9 and Fig. 10 (not Fig. 11).

Response: Revised.

Lines 515-515: Remove these lines, which belong to the caption of the figure.

Response: Revised.

Line 517: Remove "the simulation for".

Response: Revised.

Line 526: "are" → "were" (the authors have always used the past tense).

Response: Revised.

Line 527: "in" → "with respect to".

Response: Revised.

Line 527: "for" → "of".

Response: Revised.

Lines 537-540: Repetition of the word "from", possibly find a synonym somewhere.

Response: Revised.

Line 539: "THREE OTHER experimentS WERE conducted to investigate the ..." should be clearer.

Response: Revised.

Lines 545-548: Change the word "coagulation".

Response: Revised.

Line 555: "profile" → profileS".

Response: Revised.

Line 558: Remove "at 7 km", it is not needed with "In this case".

Response: Revised.

Line 559: Remove the part after "model", it is a repetition of what written before.

Response: Revised.

Line 571: No comma after "profile".

"peak" → "peakS".

Response: Revised.

Line 573: "... at lower ALTITUDES than the OBSERVED peak...".

Response: Revised.

Lines 573-574: Please, rephrase the sentence after "but".

Response: Revised.



Line 578: "... to couple the GOCART AEROSOL model TO the ...".

Response: Revised.

Line 579: "By applying this NEWLY-IMPLEMENTED microphysics scheme, ...".

Response: Revised.

Lines 580-581: Remove "by the model simultaneously with dust simulation" or explain better.

Response: Revised.

Lines 585-588: "trend" → "evolution".

"... at THE LOCATIONS OF various monitoring stations ...".

Response: Revised.

Line 589: Remove "by serving as ice nuclei".

Response: Revised.

Line 595: "... reproduced by the model over most areas of East Asia, ALTHOUGH SLIGHTLY UNDERESTIMATED." and then start a new sentence.

Remove "run".

Response: Revised.

Line 598: Remove "and the entire simulation period further", it is not correct because the sentence before refers to the IWC profiles during the dust events, along the satellite orbit or averaged along it (Fig. 9, 10, 11).

Response: Revised.

Line 601: "... calibration factor DEFINED in the DeMott2015 ...".

Response: Revised.

Lines 604: Make it simpler: "... in the model AND IS significantly ...".

Response: Revised.

Figures:

In Fig. 2, Fig. 3, Fig. 4, please, do not write the year 2012 in the tick-labels of the x-axis (to make the plot "lighter"), rather write explicitly the simulation period in the captions.

Response: Revised as suggested.

Fig.1: - try to reduce the size of blue dots or draw the contours in order to show that there are 10 dots;

- in the caption write "Blue dots represent the TEN MONITORING stations used ...";
- in the caption add the meaning of the red triangles.

Response: The size of dots has been reduced, and we also added a zoomed-in map to show the locations of all the stations, with the station name displayed in the map. However, the two stations at Jinchang are too close to each other, so they are still overlapping the other.

Fig.3: Why are there written only 5 different locations (2 per line), while in subsection 4.1 ten locations are listed? It would be clearer to write the ten different locations (one per plot).

Otherwise, if there is a reason to group the stations, it would be better to specify it in subsection 4.1.

Response: The ten stations are located at 5 cities, each city has two stations (with different station code such as XCNAQ77 at Baotou), we grouped the stations by cities. In Figure 3, the station codes as well as the city they are located at are displayed in each figure. We have clarified the reason we grouped the stations in subsection 6.1.1.

Table 1: Same considerations as before (write 10 locations?).

Add the units of the quantities computed in the table.

Response: See the response to the above comment. We have modified Table 1 to display the cities in the first column, and the station code in the second column.

The units have been added.

Fig.5: - is it possible to use the same projections for all plots?

- make country lines a bit thicker;
- near the word AOD (along the color bars), "MODIS", "MISR" and "modeled" could be added (as subscript?);
- the wavelength of MISR should be 555 instead of 550.

Response: We have replotted the plots with the same projection and thicker country lines.

Fig.6: Wrong unit in 6b.

Response: Revised.

Fig.8: - is it possible to use the same projections for all plots?

- make country lines a bit thicker.

Response: We have removed the figure, see the response to minor comment on Lines 437-440.

Fig.9 and 10: - increase the blank space between the two columns of plots;

- write the quantity (IWC) besides the unit (near the color bar);
- what do the red rectangles indicate? They are never used in the text for the explanations, I think they could be removed;

- make country lines a bit thicker;
- It would be nice to plot also the orographic profile (to explain the white areas below the GNIFA values).

Response: The blank space has been added.

IWC has been added.

The red rectangles have been removed.

The country lines have been thickened.

The orographic profiles have been added in the GNIFA profiles.

Fig.11,12,13: - write "DURING the dust events ..";

- "MEAN vertical profiles OF THE observed ice water content from CALIPSO and the simulated ice water content from ...".

Response: Revised.

# 1 Investigating the role of dust in ice nucleation within clouds and 2 further effects on the regional weather system over East Asia

## 3 Part I: model development and validation

4 Lin Su<sup>1</sup>, and Jimmy C.H. Fung<sup>2, 3</sup>

5 <sup>1</sup> School of Science, Hong Kong University of Science and Technology, Hong Kong, China

6 <sup>2</sup> Division of Environment, Hong Kong University of Science and Technology, Hong Kong, China

7 <sup>3</sup> Department of Mathematics, Hong Kong University of Science and Technology, Hong Kong, China

8 Correspondence to: Lin Su ([lsu@connect.ust.hk](mailto:lsu@connect.ust.hk))

9

10 **Keywords:** dust; ice nucleation; microphysics scheme implementation; numerical modeling

11

### 12 Highlights:

13 A new ~~microphysics scheme~~treatment has been implemented in a regional model for evaluating the role of dust  
14 particles in atmospheric ice nucleation.

15 The effect of dust on atmospheric ~~ice-water-content~~IWC over East Asia during a dust-intensive period is simulated.

16 The simulation of atmospheric ~~ice-water-content~~IWC during dust events is substantially improved upon the effect of  
17 dust being considered.

18

**Abstract.** The GOCART–Thompson microphysics scheme coupling the GOCART aerosol model and ~~the~~ aerosol-aware Thompson-~~Eidhammer~~ microphysics scheme has been implemented in WRF-Chem, to quantify and evaluate the effect of dust on the ice nucleation process in the atmosphere by serving as ice nuclei (~~IN~~). The performance of the GOCART-Thompson microphysics scheme in simulating the effect of dust in atmospheric ice nucleation is then evaluated over East Asia during spring, ~~in 2012~~, a typical dust-intensive season, ~~in 2012~~. Based upon the dust emission reasonably reproduced by WRF-Chem, the effect of dust on atmospheric cloud ice water content (~~IWC~~) is well reproduced. With abundant dust particles serving as ~~ice nuclei~~~~IN~~, the simulated ice water mixing ratio and ice crystal number concentration increases ~~by up to~~ one order of magnitude over the dust source region and downwind areas during the investigated period. The comparison with ice water path from satellite observations demonstrated that the simulation of cloud ice profile is substantially improved by ~~applying the GOCART–Thompson microphysics scheme in the simulations~~ considering the indirect effect of dust particles in the simulations. Additional sensitivity experiments are carried out to optimize the parameters in the ice nucleation parameterization in the GOCART–Thompson microphysics scheme, ~~and the results suggest that the calibration factor in the ice nucleation scheme should be set to 3 or 4~~. Results suggest that ~~Lowering~~ the threshold relative humidity to 100% for the ice nucleation parameterization leads to further improvement in cloud ice simulation.

## 36 1 Introduction

37 ~~As one of the largest natural aerosol sources, d~~Dust aerosol ~~contributes considerably~~is the second largest contributor  
38 to the global aerosol burden (Textor et al., 2006), ~~and it is estimated to contribute around 20% to the annual global~~  
39 ~~aerosol emission~~ (Tomasi et al., 2017). The Intergovernmental Panel on Climate Change (IPCC) has recognized dust  
40 as a major component of atmospheric aerosols, which are an “essential climate variable.” East Asia is ~~a a major~~main  
41 contributor to the Earth’s dust emission. It has been reported in previous studies that East Asian dust contributes 25–  
42 50% of global emission, depending on the climate of the particular year (Ginoux et al., 2001).

43 Dust in the atmosphere ~~re-ic can~~ alters the ~~Earth’s Earth’s radiation budget~~weather and climate through certain ways.  
44 By reflecting, absorbing and scattering the incoming solar radiation, dust can cause a warming effect within the  
45 atmosphere; and a cooling effect at the surface layer (Lacis, 1995), ~~which is the direct effect of dust. The semi-direct~~  
46 ~~effect of dust is related to the Dust within clouds can-absorption of b~~ short-wave and long-wave radiation ~~by dust~~  
47 ~~aerosol within clouds, leading to a warming ofand heat up~~the surrounding environment, causing a shrinking of cloud,  
48 and a lower cloud albedo, ~~and thus modifying the radiation budget~~ (Perlwitz and Miller, 2010; Hansen et al., 1997).  
49 ~~Moreover~~The dust-cloud-interaction is also referred to as the indirect effect of dust., ~~D~~e dust particles are recognized as  
50 effective ~~ice-nuclei~~IN, and play an important role in the ice nucleation process in the atmosphere, directly affecting  
51 the dynamics in ice and mixed-phase clouds, such as the formation and development of clouds and precipitation  
52 (Koehler et al., 2010; Twohy et al., 2009).

53 To date, ~~m~~Many studies have been conducted to evaluate the direct radiative effect of dust aerosol using radiation  
54 schemes implemented in numerical models all over the world (Mallet et al., 2009; Nabat et al., 2015a; Ge et al.,  
55 2010; Hartmann et al., 2013; Huang et al., 2009; Bi et al., 2013; Liu et al., 2011a; Liu et al., 2011b; Huang, 2017).  
56 Recently, semi-direct effect of dust has been investigated in a few studies over different regions by applying various  
57 global and regional models (Tsfaye et al., 2015; Nabat et al., 2015b; Seigel et al., 2013). Unfortunately, due to the  
58 poor understanding on the dust-cloud-interactions in microphysics processes, quantifying the microphysical effect of  
59 dust remains as a difficult problem. Various ice nucleation parameterizations have been implemented into global  
60 models to estimate the importance of dust in atmospheric ice nucleation (Lohmann and Diehl, 2006; Karydis et al.,  
61 2011; Hoose et al., 2008; Zhang et al., 2014). However, most regional models are not capable of estimating the indirect  
62 effect of dust, and vary rare work has been done to assess the indirect effects of dust on the weather system, especially

over East Asia, which is a major contributor to the global dust emission. Currently, only a few microphysics schemes considering aerosol-cloud-interaction are implemented in regional ~~models,~~ and ~~in~~ most of these microphysics schemes, only the cloud condensation nuclei (CCN) served by aerosols are considered (Perlwitz and Miller, 2010;Solomos et al., 2011;Miller et al., 2004), ~~with the while ice nuclei are~~ not treated, or represented by a prescribed ~~ice nuclei~~ distribution (Chapman et al., 2009;Baró et al., 2015), and the ~~production of number of predicted~~ ice crystals is ~~simplified by~~ a function of temperature or ice saturation. In reality, however, the number of ice crystals that can form in the atmosphere is highly dependent on the number of particles that can act as ~~ice nuclei~~, and dust is the most abundant aerosols that can effectively serve as ~~ice nuclei~~ and affect the formation and development of mixed-phase and ice clouds in the atmosphere. This effect should not be neglected in numerical models, especially in the simulations over arid regions during strong wind events (DeMott et al., 2003;Koehler et al., 2010;DeMott et al., 2015;Lohmann and Diehl, 2006;Atkinson et al., 2013).

~~Since~~ ~~In~~ 2014, the aerosol-aware Thompson-~~Eidhammer~~ microphysics scheme, which takes into account the aerosols serving as CCN and ~~ice nuclei~~, has been implemented into the Weather Research and Forecast (WRF) model, enabling the model to explicitly predict the ~~droplet-number concentration for cloud droplets and ice crystals through the number concentrations of cloud condensation nuclei and ice nuclei~~ (Thompson and Eidhammer, 2014). Therefore, the aerosol-aware Thompson-~~Eidhammer~~ scheme is an ideal microphysics scheme for evaluating the effect of dust in atmospheric ice nucleation processes. However, this scheme is not coupled with any aerosol model in WRF-Chem, the Weather Research and Forecast model coupled with Chemistry. ~~When the aerosol-aware Thompson-Eidhammer microphysics scheme is activated, the model reads in pre-given climatological aerosol data derived from the output of other global climate models, which introduces large errors into the estimation of the effects of dust in microphysical processes. This problem can be solved by embedding a dust scheme into Thompson-Eidhammer scheme, or couple the microphysics scheme with WRF-Chem. Compared with WRF, WRF-Chem integrates various emission schemes and aerosol mechanisms for simulating the emission, transport, mixing, and chemical transformation of aerosols simultaneously with the meteorology (Grell et al., 2013). Therefore, WRF-Chem is more capable of producing a realistic aerosol field by comparing the performances of different emission schemes or aerosol mechanisms. When the aerosol-aware Thompson-Eidhammer microphysics scheme is activated, the model reads in pre-given climatological aerosol data derived from the output of other global climate models, which introduces large errors into the estimation of the effects of dust in microphysical processes.~~

In light of ~~the~~ above, we aimed to fully couple the aerosol-aware Thompson-~~Eidhammer~~ microphysics scheme with ~~an aerosol model~~ the Goddard Chemistry Aerosol Radiation and Transport (GOCART) model (Ginoux et al., 2001) in the WRF-Chem modeling system in this study, enabling ~~the model~~ WRF-Chem to simultaneously simulate the effect of dust aerosol in ice nucleation processes during ~~online~~ simulations. Based upon the implementation, the performance of the coupled GOCART-Thompson microphysics scheme in simulating the ice nucleation process involving dust particles was validated, for and investigating the role that East Asian dust plays in the ice nucleation process in the atmosphere was further investigated.

The remainder of the manuscript is presented as follows. Section 2 provides a description of the model including the implementation work for coupling the aerosol-aware Thompson-~~Eidhammer~~ microphysics scheme and the GOCART aerosol model in WRF-Chem, followed by the model configurations for numerical simulations in section 3. Section 4 presents the observational data used to validate the performance of the ~~newly implemented~~ GOCART-Thompson microphysics scheme. Section 5 is the results and discussion, followed by the conclusions in section 6.

## 2 Model description

WRF-Chem is an online-coupled regional modeling system, which means that it can simultaneously simulate the meteorological field, the chemical field, and the interactions in between (Grell et al., 2013). The chemical model contains several gas- and aerosol-phase chemical schemes. In this study, we focus on the GOCART model, a simple aerosol model that will be used for dust simulation.

### 2.1 GOCART aerosol model

GOCART is an aerosol model for simulating major tropospheric natural-source aerosol components, such as sulfate, mineral dust, black carbon, organic carbon, and sea-salt aerosols (Ginoux et al., 2001; Chin et al., 2000). It has been implemented into WRF-Chem as a bulk aerosol scheme. GOCART is a simple aerosol scheme that can predict the mass of aerosol components, but does not account for complex chemical reactions. Therefore, it is numerically efficient in simulating aerosol transport, and thus applicable to cases without many chemical processes, especially



116 dust events. [Typically it requires 40% to 50% more computational time by applying WRF-Chem run with GOCART](#)  
117 [aerosol model than the standard WRF to produce the same period of simulation.](#)

118 Shao's dust emission scheme [model \(Kang et al., 2011;Shao, 2004, 2001;Shao et al., 2011\)](#) is one of the ~~three~~ dust  
119 emission schemes in the GOCART aerosol ~~model (Kang et al., 2011;Shao, 2004, 2001;Shao et al., 2011)~~, and has  
120 been demonstrated to exhibit superior performance in reproducing the dust cycle over East Asia compared to other  
121 emission schemes (Su and Fung, 2015). The Shao's emission scheme was updated in WRF-Chem since version 3.8  
122 released in 2016, to produce five size bins for dust emission, with diameters of < 2  $\mu\text{m}$ , 2–3.6  $\mu\text{m}$ , 3.6–6.0  $\mu\text{m}$ , 6.0–  
123 12.0  $\mu\text{m}$ , and 12.0–20.0  $\mu\text{m}$ , and mean effective radii of 0.73  $\mu\text{m}$ , 1.4  $\mu\text{m}$ , 2.4  $\mu\text{m}$ , 4.5  $\mu\text{m}$ , and 8.0  $\mu\text{m}$ .

124

## 125 2.2 Aerosol-aware Thompson microphysics scheme

126 The Thompson scheme is a bulk two-moment microphysics scheme that considers the mixing ratios and number  
127 concentrations for five water species: cloud water, cloud ice, rain, snow and a hybrid graupel/hail category (Thompson  
128 et al., 2004). The ~~aerosol-aware version of the~~ Thompson-Eidhammer scheme ~~is an aerosol-aware version of the~~  
129 ~~Thompson scheme~~ (Thompson and Eidhammer, 2014). ~~It~~ incorporates the activation of aerosols serving as cloud  
130 condensation nuclei and ~~ice nuclei~~IN, and therefore it explicitly predicts the ~~droplet~~-number concentration~~s~~ of ~~cloud~~  
131 ~~water as well as the number concentrations of cloud condensation nuclei- CCN and ice nuclei~~IN, as well as the number  
132 ~~concentrations of cloud droplets and ice crystals~~. Hygroscopic aerosols that serve as cloud condensation nuclei are  
133 referred to as water-friendly aerosols, and those non-hygroscopic ice-nucleating aerosols are referred to as ice-friendly  
134 aerosols. The cloud droplets nucleate from explicit aerosol number concentration~~s~~ using a look-up table for the  
135 activated fraction as determined by the predicted temperature, vertical velocity, number of available aerosols, and pre-  
136 determined values of the hygroscopicity parameter and aerosol mean radius~~s~~.

137 [The parameterization for condensation and immersion freezing in the aerosol-aware Thompson-Eidhammer](#)  
138 [microphysics scheme was proposed in 2010 \(DeMott et al., 2010, hereafter referred to as the DeMott2010 scheme\)](#)  
139 [based on combined data from field experiments at a variety of locations over 14 years. In the Demott2010](#)  
140 [parameterization, the relationship between the number concentration of aerosol-friendly aerosols and ice nucleating](#)  
141 [particles \(INP\) is as follows:](#)

Field Code Changed

Field Code Changed

$$n_{IN,T_k} = a(273.16 - T_k)^b n_{aero}^{(c(273.16 - T_k) + d)} \quad (1)$$

where  $n_{IN,T_k}$  is the ice crystal number concentration at temperature of  $T_k$ ;  $n_{aero}$  is the number concentration of ice-friendly aerosols, and  $a$ ,  $b$ ,  $c$ , and  $d$  are constant coefficients equal to  $5.94 \times 10^{-5}$ , 3.33,  $2.64 \times 10^{-2}$ , and  $3.33 \times 10^{-3}$ , respectively. The parameterization was tested with various temperatures and number concentration of ice-friendly aerosols, yielding a good performance in reproducing ice crystal number concentration under conditions of relatively low mixing ratio of water vapor or low concentration of INP compared with field-experimental data. The relationship between the simulated number concentrations of ice-friendly aerosols and INP is basically linear for concentrations of both of under  $1,000 \text{ \#/cm}^3$  (DeMott et al., 2010).

The above parameterization was further developed in 2015 (DeMott et al., 2015, hereafter the DeMott2015 scheme) for conditions of higher mixing ratio of water vapor or higher concentrations of ice crystals based on the latest data from field and laboratory experiments. According to the updated observational data, INP concentration increases exponentially with number concentration of ice-friendly aerosols, and existing aerosols with relatively low concentrations (less than  $1,000 \text{ \#/cm}^3$ ) can produce a large number of INP (more than  $100,000 \text{ \#/cm}^3$ ). The updated relationship between the number concentrations of ice-friendly aerosols and INP in the DeMott2015 parameterization scheme is as follows.

$$n_{IN,T_k} = c_f n_{aero}^{\alpha(273.16 - T_k) + \beta} \exp(\gamma(273.16 - T_k) + \delta) \quad (2)$$

where  $\alpha$ ,  $\beta$ ,  $\gamma$ , and  $\delta$  are constant coefficients equal to 0, 1.25, 0.46, and -11.6, respectively. The calibration factor  $c_f$  ranges from 1 to 6, and is recommended to be 3.

The number concentration of INP produced by the DeMott2015 scheme is much higher than that produced by the DeMott2010 scheme, and the difference grows larger with decreasing temperature and increasing number concentration of ice-friendly aerosols (DeMott et al., 2015). As the DeMott2015 scheme has been examined using more comprehensive field- and laboratory-experimental data, we apply the DeMott2015 ice nucleation scheme in the GOCART-Thompson microphysics scheme to be implemented, instead of the DeMott2010 scheme, in the default aerosol-aware Thompson-Eidhammer microphysics scheme to simulate the ice nucleation involving dust.

Originally, the calibration factor  $c_f$  is set to be 3; the threshold temperature is set to be  $-20 \text{ }^\circ\text{C}$ . The ice nucleation process is triggered once the relative humidity with respect to ice ( $RH_i$ ) exceeds 105%. Furthermore, when the relative

humidity with respect to water ( $RH_w$ ) is above 98.5%, it is counted as condensation and immersion freezing, and calculated by DeMott2015 scheme; when  $RH_w$  is below 98.5%, it is treated as deposition nucleation, and determined by the while (The nucleation of ice crystals by dust particles follows the parameterization of DeMott et al. (DeMott et al., 2010) to account for condensation and immersion freezing, and the parameterization of Phillips et al. (Phillips et al., 2008) is applied to account for deposition nucleation.

In addition, the freezing of deliquesced aerosols using the hygroscopic aerosol concentration is parameterized following Koop et al. (Koop et al., 2000), with the background aerosol concentration set to be 1 /L. In the current version of WRF-ChemFor the Thompson-Eidhammer scheme in WRF, the number concentrations of both water-friendly aerosols and ice-friendly aerosols are pre-given in the initialization of the simulations, and are derived from the climatological data produced by global model simulations in which particles and their precursors are emitted by natural and anthropogenic sources and explicitly modeled with multiple-various size bins for multiple species of aerosols by the GOCART model. In the consequent simulations, a fake aerosol emission is implemented by giving a variable lower boundary condition based on the initial near-surface aerosol concentration and a simple mean surface wind for calculating a constant aerosol flux at the lowest level in the model. The number concentrations of both water-friendly aerosols and ice-friendly aerosols are then updated at every time step by summing up the fake aerosol emission fluxes and tendencies induced by aerosol-cloud-interactions. The limitation of the current aerosol-aware Thompson-Eidhammer scheme is that the aerosol profile generated from a fake emission can not-hardly represent the realistic aerosol level all the time, especially over areas with complex weathers, such as East Asia, leading to great errors in quantifying the indirect effects of aerosols.

By coupling the GOCART aerosol model with the Thompson-Eidhammer microphysics scheme, it allows the model to explicitly evaluate the indirect effect of natural-source aerosols on the basic of a relatively realistic emission production, for instance, the effect of dust on ice nucleation during severe dust episodes or dust-intensive season.

### 2.3 Implementation of GOCART-Thompson microphysics scheme

To investigate the real-time indirect effects of dust aerosol over East Asia, modifications have been made to couple the GOCART model with the aerosol-aware Thompson-Eidhammer microphysics scheme. The modifications were

based on WRF-Chem version 3.8.1, and consisted of three parts, modification of the GOCART aerosol scheme, modification of the aerosol-aware Thompson microphysics scheme, and the introduction of a new wet removal scheme. To investigate the real-time indirect effects of dust aerosol over East Asia, a new treatment was implemented into WRF-Chem to couple the GOCART aerosol model has been coupled to and the Thompson-Eidhammer microphysics scheme, namely GOCART-Thompson microphysics scheme. To accomplish this, WRF-Chem version 3.8.1 has been modified in the following three steps.

### 2.3.1 Upgraded GOCART aerosol model

Currently, the GOCART aerosol model generates only the mass concentration for aerosols but no number concentrations. However, the number concentrations of aerosols are required for a microphysics scheme to evaluating the indirect effects of aerosols. Therefore, modification was needed to provide information about the number concentrations of aerosols from the mass concentration produced in GOCART aerosol model.

The aerosol mass concentration was converted into number concentration using the aerosol density and effective radius for each size bin. Assuming that dust particles are spherical, the mass per dust particle ( $m_p$ ,  $\mu\text{g}/\#$ ) for a size bin can be approximated through the mean effective radius ( $r_{dust, m}$ ) and density ( $\rho_{dust, kg/m^3}$ ) for that size bin.

$$m_p = \rho_{dust} \times \frac{4}{3} \times \pi r_{dust}^3 \quad (41)$$

The aerosol-number concentration of dust particles  $N$  ( $\#/\text{kg}$ ) for size bin  $n$  at a grid point  $(i, j, k)$  is then calculated by the following equation:

$$N(i, j, k, n) = C(i, j, k, n) / m_p \quad (42)$$

where  $C(i, j, k, n)$  is the dust mass mixing ratio ( $\mu\text{g}/\text{kg}$ ) for size bin  $n$  at grid point  $(i, j, k)$ . Summing up the aerosol number concentrations through all of the size bins gives a total dust number concentration, which will be passed into the Thompson-Eidhammer microphysics scheme. Note that all of the dust particles are treated as ice-friendly aerosols in this study, and represented by a newly-introduction variable, ice-friendly aerosol produced by GOCART aerosol model (*GNIFA*).

$$GNIFA(i, j, k) = \sum_{n=1}^n N(i, j, k, n) \quad (53)$$

Formatted: Superscript

where  $n_{ice,T_k}$  is the ice crystal number concentration at temperature of  $T_k$ ;  $n_{aero}$  is the number concentration of ice-

### 2.3.23 GOCART-Thompson microphysics scheme

This part of modification was to hoop up the GOCART aerosol model and the Thompson-Eidhammer microphysics scheme. Firstly, the initialization module for the aerosols in the aerosol-aware Thompson-Eidhammer scheme was modified. The initialization module used to read in pre-given climatological aerosol data at the first time step of the simulation, which provided an annual mean of the global distribution of the number concentrations of the water-friendly and ice-friendly aerosols in the aerosol-aware Thompson-Eidhammer microphysics scheme. In the updated GOCART-Thompson microphysics scheme, the initialization module was removed, instead, the scheme was modified to read in the bulk number concentration of aerosols produced by the GOCART aerosol model updated at every time step.

Secondly, instead of reading in the pre-given climatological aerosol data, the initialization module of the Thompson-Eidhammer microphysics scheme was modified to apply the bulk number concentration of ice-friendly aerosols read in from produced by the GOCART aerosol model is passed into the updated GOCART-Thompson microphysics scheme for the calculation of the number concentration of ice nucleating particles.

After the microphysical processes are finished for a particular time step, the tendency of term ( $ten_{dust}$ , #/kg/s) for the bulk aerosol number concentration ( $ten_{dust}$ , #/kg/s) produced by the microphysics scheme is then passed into a wet scavenging scheme, which will be described in detail in the following subsection, for the model to calculate the loss of aerosol mass due to the microphysical processes within clouds, and update the aerosol mass field.

### 2.3.34 In-cloud wet scavenging

As no in-cloud scavenging is considered for dust aerosol in WRF-Chem, a new wet scavenging process was then introduced into WRF-Chem to calculate the loss of aerosol mass due to the microphysical processes within clouds using the tendency of aerosol number concentration produced by the microphysics scheme. Assuming that the collection of dust particles is proportional to the number concentration of dust particles, the fraction of dust particle for each size bin ( $\varphi$ , %) can be calculated in the GOCART aerosol model:

$$\varphi(i, j, k, n) = \frac{N(i, j, k, n)}{GNIFA(i, j, k)} \quad (6)$$

The tendency of ice-friendly aerosol is then distributed into each size bin and the loss of dust mass due to the microphysical processes (*wetscav*,  $\mu\text{g/kg}$ ) for a particular size bin  $n$  is calculated by the following equation:

$$wetscav(i, j, k, n) = ten_{dust}(i, j, k) \times \varphi(i, j, k, n) \times m_p \times dt \quad (7)$$

where  $dt$  is the time step for the simulation.

The mass mixing ratio ( $C$ ,  $\mu\text{g/kg}$ ) for dust aerosol in a particular size bin  $n$  is then updated ~~for the following simulation~~

$$C_{(i,j,k,n)}^{t+1} = C_{(i,j,k,n)}^t - wetscav_{(i,j,k,n)}^t \quad (8)$$

Apart from the in-cloud scavenging, the below-cloud wet removal is calculated by the default wet deposition scheme in the GOCART aerosol model, in which the wet removal of dust is ~~proportional to concentration removed by a~~ constant scavenging factor when there is a precipitation (Duce et al., 1991; Hsu et al., 2009).

#### 4.3 Model configurations

A numerical experiment was conducted to examine the performance of the newly-implemented GOCART–Thompson microphysics scheme in simulating the ice nucleation process induced by dust in the atmosphere. Two simulations were conducted for the numerical test. One control run (CTRL) was conducted without dust and one test run (DUST) was conducted with dust. According to the observations, the dust events in 2012 over East Asia were concentrated in mid-March to late-April, and the satellite observations from mid-March to the end of April were available for model validation; therefore, the simulation period ~~for this numerical test~~ was from March 9 to April 30, 2012, with the first eight days as “spin-up” time. Only the results from March 17 to April 30, 2012 were used for ~~further the~~ analysis. The final reanalysis data provided by the United States National Center of Environmental Prediction with a horizontal resolution of one degree was used for generating the initial and boundary conditions for the meteorological fields, and the simulations were re-initialized every four days, with the aerosol field being re-cycled, which means that the output

of the aerosol field from the previous four-day run was used as the initial aerosol state for the subsequent four-day run. The integration time step for the simulations was 90s.

Two nested domains were used for the simulations, as shown in Figure 1. The outer domain (domain 1) is in a horizontal resolution of 27 km, and covers the entire East Asia region. The inner domain (domain 2) is in a horizontal resolution of 9 km, and covers the entire central to East China. Both domains have 40 vertical layers, with the top layer at 50 hPa. The locations of the two major dust sources, the Taklimakan Desert (TD) and the Gobi Desert (GD), are marked in Figure 1.

~~Two simulations were conducted for the numerical test. One control run (CTRL) was conducted without dust and one test run (DUST) was conducted with dust. The GOCART aerosol model was applied to simulate aerosol processes (Ginoux et al., 2001; Ginoux et al., 2004). Shao's dust emission (Kang et al., 2011; Shao et al., 2011) with soil data from the United States Geological Survey (Soil Survey Staff, 1993), which have been demonstrated to have good performance in reproducing dust emissions over East Asia, was used to generate dust emission in the test run. No other aerosol emissions were considered in the simulations. both using the newly-implemented GOCART-Thompson microphysics scheme. In the GOCART-Thompson scheme, the deposition nucleation is determined by the parameterization of Phillips et al. (Phillips et al., 2008), the freezing of deliquesced aerosols using the hygroscopic aerosol concentration is parameterized following Koop et al. (Koop et al., 2000), with the background aerosol concentration set to be 1/L, and the condensation and immersion freezing is parameterized by the DeMott2015 ice nucleation scheme. The GOCART aerosol model was applied to simulate aerosol processes (Ginoux et al., 2001; Ginoux et al., 2004). Shao's dust emission (Kang et al., 2011; Shao et al., 2011) with soil data from the United States Geological Survey (Soil Survey Staff, 1993), which have been demonstrated to have good performance in reproducing dust emissions over East Asia were used to generate dust emission in the test run. The new wet scavenging scheme was used for in-cloud wet scavenging of aerosols due to microphysical processes.~~

~~Other important physical and chemical parameterizations applied for the simulations are as follows. The Mellor-Yamada-Janjic (MYJ) turbulent kinetic energy scheme was used for the planetary boundary layer parameterization (Janjic, 2002, 1994); the moisture convective processes were parameterized by the Grell-Freitas scheme (Grell and Freitas, 2014); the short-wave (SW) and long-wave (LW) radiation budgets were calculated by the Rapid Radiative Transfer Model for General Circulation (RRTMG) SW and LW radiation schemes (Mlawer et al., 1997; Iacono et al.,~~

2008); the gravitational settling and surface deposition were combined for aerosol dry deposition calculation (Wesely, 1989); a simple washout method was used for the below-cloud wet deposition of aerosols (Duce et al., 1991; Hsu et al., 2006); and the aerosol optical properties were calculated based on the volume-averaging method (Horvath, 1998).

## 5.4 Observations

### 5.4.1 Surface PM<sub>10</sub> observations

The hourly observations of surface concentration of particulate matter with diameter smaller than 10  $\mu\text{m}$  (PM<sub>10</sub>) ~~concentration~~ at ten environmental monitoring stations located in or surrounding the dust source areas in East Asia were used to examine the capability of the model in reproducing ~~the trend and magnitude of~~ dust levels at the ground surface during the simulation period. The ten stations (indicated by blue dots in Figure 1) were located in the following five cities: Jinchang, Gansu Province, Yinchuan, Qinghai Province, Shizuishan, Ningxia Province, Baotou, Inner Mongolia, and Yan'an, Shaanxi Province, with two stations in each city. ~~The location of the ten stations are indicated by the blue dots in Figure 1.~~

### 5.4.2 AERONET AOD observations

The AERONET program is a ground-based aerosol remote sensing network for measuring aerosol optical properties at sites distributed around the globe. This program provides a long-term database of aerosol optical properties such as aerosol extinction coefficient, single-scattering albedo, and aerosol optical depth (AOD) measured at various wavelength. ~~The AOD represents the total amount of aerosols within the atmospheric column.~~ The observational data from two sites were available for comparison with the simulation results during the simulation period in this study. One was Dalanzadgad located to the north of the Gobi Desert in Mongolia, and the other was the Semi-Arid Climate and Environment Observatory of Lanzhou University (SACOL) located at Lanzhou, Gansu Province, China. The exact locations of the two AERONET sites are depicted by the red triangles in Figure 1. All of the measured data had passed the quality control standard level 2, with an uncertainty of  $\pm 0.01$  (Holben et al., 2001).



### 5.4.3 Satellite data

#### 5.4.3.1 Multi-angle Imaging SpectroRadiometer (MISR)

The MISR instrument aboard the Terra platform of the United State National Aeronautics and Space Administration (NASA) has been monitoring aerosol properties globally since 2000. It ~~observes~~measures the aerosol properties in four narrow spectral band centered at 443 nm, 555 nm, 670 nm, and 865 nm, due to which the aerosol properties even over highly bright surfaces, such as deserts, can be retrieved (Martonchik et al., 2004; Diner et al., 1998). In this study, the AOD data at 555 nm retrieved from the MISR level 3 products with a spatial resolution of 0.5° were used for comparison with the spatial distribution of simulated AOD over East Asia during the investigated period.

#### 5.4.3.2 Moderate Resolution Imaging Spectroradiometer (MODIS)

The MODIS instruments aboard Terra and Aqua platforms of NASA monitor Earth's changes~~surface~~ and provide global high-resolution cloud and aerosol optical properties at a near-daily interval (Kaufman et al., 1997).

To retrieve aerosol information over bright surfaces, ~~such as deserts~~, the Deep Blue algorithm was developed to employ retrievals from the blue channels of the MODIS instruments, at which wavelength the surface reflectance is very low, such that the presence of aerosol can be detected by increasing total reflectance and enhanced spectral contrast (Hsu et al., 2006). By applying this algorithm, the AOD values at wavelengths of 214 nm, 470 nm, 550 nm, and 670 nm over bright surfaces can be retrieved. In this study, the MODIS level 2 AOD data at ~~550~~ nm with a spatial resolution of 10 km were used for comparison with the simulated AOD during the simulation period.

~~Furthermore, MODIS combines infrared and visible techniques to detect physical and radiative cloud properties, and a near-infrared algorithm was applied to retrieve the precipitable water vapor, including liquid and ice water content (IWC), in the atmosphere (Gao and Kaufman, 1998). The thermal column water vapor path was then derived by integrating the moisture profile throughout the atmospheric column. In this study, the ice water path retrieved from the MODIS level 3 cloud products with a spatial resolution of one degree was used for comparison with simulated ice water path during the simulation period.~~

#### 5.4.3.3 Cloud-Aerosol Lidar and Infrared Pathfinder Satellite Observation (CALIPSO)

The Cloud-Aerosol Lidar and Infrared Pathfinder Satellite, which is aboard the Aqua platform of NASA, combines an active Light Detection and Ranging (LIDAR) instrument with passive infrared and visible imagers to probe the vertical structure and properties of thin clouds and aerosols around the globe (Vaughan et al., 2004). It aims to fill existing gaps in the ability to measure the global distribution of aerosols and cloud properties, and provides three-dimensional perspectives of how clouds and aerosols form, evolve, and affect weather and climate. It ~~measures~~observes high-resolution vertical profiles of aerosol and cloud extinction coefficient globally at wavelengths of 532nm and 1064 nm. The atmospheric ~~ice-water-content~~(IWC) is derived from the observational cloud extinction coefficients at 532 nm (Winker et al., 2009). In this study, the vertical profiles of CALIPSO IWC with a horizontal resolution of 5 km and vertical resolution of 60 m were applied to verify the performance of the model in simulating the vertical distribution of atmospheric ~~ice-water-content~~IWC.

## **6.5 Results and model validation**

### **6.5.1 Dust over East Asia**

The time series of daily average dust load over the entire East Asia region (domain 1) during the simulation period is shown in Figure 2a. In total four dust events occurred during the simulation period, lasting from March 18 to 25, March 30 to April 7, April 9 to 19, and April 22 to 29, 2012. The case from April 22 to 29 was the most significant one, with daily ~~s~~ dust ~~mass~~-load ~~that of~~double as the other cases. The fraction of daily dust load for each size bin is also shown in Figure 2a. The dust particles in the ~~third~~, fourth and fifth bins with effective diameters ranging from ~~3.6~~ to 20  $\mu\text{m}$  account for ~~the major part~~around 60% of the total mass of dust aerosols, and dust particles with diameters smaller than ~~3.6~~  $\mu\text{m}$  account for ~~a minor fraction~~around 40% of the total mass of dust aerosols.

~~The number concentration of dust particles over East Asia were vertically integrated to obtain the number density of dust particles. As shown in Figure 2b, t~~The time series of the daily average number density of dust particles over East Asia during the simulation period ~~shown in Figure 2b~~ shows a similar distribution as that for dust load; the noteworthy distinction between the ~~two~~ time series ~~for dust load and number density~~ lies in the fraction of each size bin. The two size bins with the smallest diameters (no larger than 3.6  $\mu\text{m}$ ) account for over 80% of the total number of dust particles, and the particles with diameters smaller than 6  $\mu\text{m}$  account for over 95% of the total number of dust particles,

indicating that the smallest dust particles are the main source of ice-friendly aerosol to serve as ~~ice-nuclei~~<sup>IN</sup> in the

#### 6.1.1 Surface PM<sub>10</sub> concentration

To evaluate the performance of WRF-Chem in reproducing dust emissions over East Asia, the simulated surface PM<sub>10</sub> concentrations were compared with the observations from the ten environmental monitoring stations located near dust sources and downwind areas (described in subsection Section 5.1). The time series of the observed and simulated surface PM<sub>10</sub> concentrations at the ten stations during the simulation period are shown in Figure 3. Note that the concentration were extracted from the nearest grid point to the geographical coordinates of the stations. The stations in the same city were assigned into one group, thus here were five groups in Figure 3. Overall, the model shows a good performance in simulating the dust cycle at different stations/locations, with evolution and the trend and PM<sub>10</sub> concentration well captured at most of the stations, although the surface PM<sub>10</sub> concentration was overestimated concentration than those observed, as no other emissions were considered in the simulations. However, the dust events on March 21 and April 26 were overestimated by the model at one station in Jinchang (Figure 3e), and the dust event Shizuishan (Figure 3c and d) and Yinchuan (Figure 3i and j).

The performance statistics were computed from the daily average simulated PM<sub>10</sub> concentration from DUST and the corresponding observations, for the simulated results are as shown in Table 1. The model tends to produce lower surface PM<sub>10</sub> concentrations than those observed, as no other emissions were considered in the simulations. The mean bias (MB) ranged from  $-108.73 \mu\text{g}/\text{m}^3$  to  $72.46 \mu\text{g}/\text{m}^3$ , with a mean over all of the stations of  $-18.84 \mu\text{g}/\text{m}^3$ . The mean error (ME) ranged from  $46.07 \mu\text{g}/\text{m}^3$  to  $155.83 \mu\text{g}/\text{m}^3$ , with a mean over all of the stations of  $107.24 \mu\text{g}/\text{m}^3$ . The root mean squared error (RMSE) ranged from  $64.78 \mu\text{g}/\text{m}^3$  to  $317.73 \mu\text{g}/\text{m}^3$ , with a mean over all of the stations of  $181.28 \mu\text{g}/\text{m}^3$ . The relatively large values of the MB, ME and RMSE are mainly attributed to the fact that no other aerosol emissions were considered in the simulations other than dust, while the surface PM<sub>10</sub> concentration at the monitoring stations is influenced by aerosols emitted from other sources, such as anthropogenic emissions. The correlation coefficient (r) ranged from 0.59 to 0.87, with an average for all of the stations of 0.70. The comparisons between the observed and simulated surface PM<sub>10</sub> concentration indicates that the model is capable of reproducing the surface dust concentration reasonably during dust events over East Asia.

396

### 397 6.5.1.2 AOD time series

398 To examine the performance of the model in reproducing the column sum of dust in the atmosphere, the simulated  
399 AOD values were compared with observations measured at two AERONET sites during the simulation period, as  
400 shown in Figure 4.

401 The site at Dalanzadgad (Figure 4a) is located in Mongolia to the north of the Gobi Desert. Overall, the evolution and  
402 magnitude of the AOD time series at Dalanzadgad were reasonably reproduced by the model during the simulation  
403 period. Despite the fact that the simulated AOD was overestimated at the end of March and in mid-April compared  
404 to the observed values, ~~the trend and magnitude of the AOD time series at Dalanzadgad was reasonably reproduced~~  
405 ~~by the model during the simulation period.~~

406 SACOL (Figure 4b) is a site located in Lanzhou, Gansu Province, which is a typical downwind area for dust in China.  
407 The model showed a good performance in reproducing the time series of AOD at SACOL during the entire simulation  
408 period, with evolution and magnitude of AOD well captured. ~~Apart from the overestimation on April 23, the model~~  
409 ~~showed a good performance in reproducing the time series of AOD at SACOL during the entire simulation period,~~  
410 ~~with the trend and magnitude of AOD well captured.~~

411

### 412 6.5.1.3 Satellite-observational AOD spatial distribution

413 The spatial distribution of monthly mean simulated AOD ~~during the simulation period~~ was also compared with  
414 observed values from MODIS and MISR products. Note that the high AOD values observed at North, East, South  
415 China and part of Southeast Asia are attributed to the abundant anthropogenic emissions, while those high values in  
416 the circle area are mostly due to dust events. ~~T~~The region with high AOD values in the west part of the circled area is  
417 TD, and the region with relatively lower AOD in the east part of the circled area is GD. The AOD observed by MODIS  
418 showed high values at the dust source region in both March and April of 2012, as shown in Figures 5a and b. ~~The~~  
419 ~~region with high AOD values in the west part of the circled area is the Taklimakan Desert, and the region with~~  
420 ~~relatively lower AOD in the east part of the circled area is the Gobi Desert.~~ The mean observed AOD over ~~the Gobi~~  
421 ~~Desert~~GD was lower than that over ~~the Taklimakan Desert~~TD in both March and April, and the mean observed AOD

was higher in April than in March over both dust source areas. The spatial patterns of AOD observed by MISR are similar to MODIS, with comparable mean values over the Gobi Desert GD. However, the mean AOD significantly lower values over the Taklimakan Desert TD observed by MISR are over 36%–50% and 40% lower than those by MODIS in both March and April, respectively (Figure 5c and d).

The spatial patterns for the mean simulated AOD were similar to the observed values for the observations in both months but closer to those from MODIS, as shown in Figures 5e and f. The model shows a good capability in capturing the spatial characteristics of the AOD, as well as the trend in AOD from March to April over the dust source areas. For example, the mean observed AOD was higher in the southern part of the Taklimakan Desert TD was higher than that in the northern part in March, and the mean AOD showed an increase from March to April over the Gobi Desert GD, both of which were captured by the model. The values of the mean simulated AOD over the Gobi Desert (0.33 for March and 0.39 for April) are comparable to the observational values from both MODIS (0.30 for March and 0.32 for April) and MISR (0.31 for March and 0.34 for April), but the mean simulated AOD over the Taklimakan Desert TD (0.54 for March and 0.64 for April) are between the values of the MISR observations (0.72 for March and 0.88 for April) and the MODIS observations (0.46 for March and 0.53 for April).

In summary, it was demonstrated that the dust emissions simulated by WRF-Chem are reliable for further analysis by the comparison between the simulation results and the observations for surface PM<sub>10</sub> concentrations, as well as the temporal and spatial distributions of AOD values.

## 6.5.2 Cloud ice over East Asia

Dust particles are effective ice nuclei IN and play an important role in ice nucleation in the atmosphere under appropriate conditions. With the large number of ice nuclei IN served by dust particles emitted into the atmosphere, an increase in the number of ice crystals is expected in the results from DUST compared with those from CTRL, after taking into account the effects of dust particles in the GOCART–Thompson microphysics scheme, as the ice nucleation process is supposed to be enhanced by dust particles at appropriate temperature and relative humidity, as shown by Figure 6 shows the overall comparison between the simulated cloud ice mixing ratio and ice crystal number

concentration at each simulated data point (at all model grids at hourly intervals) from CTRL and DUST during the entire simulation period in Figure 6.

As expected, the model produces a much higher cloud ice mixing ratio (Figure 6a) and ice crystal number concentration (Figure 6b) in DUST. The simulated cloud ice mixing ratio produced in CTRL is lower than  $2 \mu\text{g/kg}$  at most data points during the simulation period, whereas the data points with simulated ice mixing ratio higher than  $2 \mu\text{g/kg}$  are substantially increased in the output of DUST. Similarly, the simulated ice crystal number concentration produced in CTRL is lower than  $0.5 \times 10^6 \text{ \# / kg}$  at most data points during the simulation period, by contrast, the simulated ice crystal number concentration is higher than  $0.5 \times 10^6 \text{ \# / kg}$  at over a half of total data points in DUST. The substantial increase of simulated cloud ice mixing ratio and ice crystal number concentration indicates that the enhancement of ice nucleation process induced by dust is successfully reproduced by the newly-implemented GOCART-Thompson microphysics scheme during the simulation period.

#### 6.2.1 Spatial distribution of ice water path (IWP)

The spatial distributions of the simulated ~~ice water path~~IWP and ice crystal number density from CTRL and DUST in Figure 7 further demonstrate the ~~spatial pattern of the~~ enhancement in cloud ice due to dust over East Asia. The ~~ice water path~~IWP produced by CTRL was lower than  $1 \text{ g/m}^2$  over the entire East Asia Region (Figure 7a). After considering the effect of dust in the ice nucleation process, the ~~ice water path~~IWP produced by DUST increased substantially over the entire region, especially over dust sources and downwind areas, with values as high as  $10 \text{ g/m}^2$  (Figure 7b and c). ~~The ice water path was increased by one order of magnitude as a result of the effect of dust particles serving as ice nuclei in the atmosphere.~~ The mean IWP averaged over the domain during the simulation period was ~~CTRL~~. As shown in Figures 7d–f, the spatial pattern for the enhancement of ice crystal number density over East Asia was similar with that for the ~~ice water path~~IWP. ~~The mean ice crystal number density averaged over the domain during period was  $2.79 \times 10^8 \text{ /m}^2$  for DUST, and  $6.38 \times 10^6 \text{ /m}^2$  for CTRL.~~

The IWP and ice crystal number density ~~were~~was increased by ~~more than~~ one order of magnitude over vast areas of East Asia upon considering the effect of dust in the ice nucleation process in the simulation, ~~and such effect can reach as far as the South China Sea at the southern part of the simulation domain (Figure 7b and 7e). During dust season,~~

the outbreak of cold high system over northeast Asia can bring quantitative dust aerosol down to the South China Sea or even further. In such cases, strong northwestlies swept across the entire China, and brought large amount of dust, especially fine particles, from source areas to the south border of the domain. Besides, the water vapor mixing ratio over South China Sea can be several times as that over north China. Large amount of ice nuclei transported by winds, combining with abundant water vapor, results in a substantial enhancement in the formation of ice crystals over the area at the southern part of the simulation domain. The larger fraction of fine particles in the dust plumes that reach this area results in a much higher enhancement of ice crystal number concentration than the mass of ice crystals.

#### 5.2.1 Ice water path (IWP)

#### 5.2.2 Ice water content (IWC) during dust events

The vertical profile of the simulated ice water content (IWC) was also compared with the observation from CALIPSO during dust events. As mentioned in section 5.1, a total of four dust events occurred during the simulation period, lasting from March 18 to 25, March 30 to April 7, April 9 to 19, and April 22 to 28, 2012. As shown in Figures 899 and 940, the performance of the model in simulating the vertical profile of IWC was evaluated by comparing the simulated vertical profiles of the ice water content (IWC) during each dust events were compared with the observationss measured at 06 UTC on March 21, 18 UTC on April 1, 18 UTC on April 9, and 05 UTC on April 23, 2012 with the simulated profiles at the same hour, when the orbit of the satellite passed over East Asia.

Unlike the MODIS ice water path (IWP), CALIPSO measures the global distribution of aerosol and cloud properties by LIDAR, which uses a laser to generate visible light with a wavelength of 1  $\mu\text{m}$  or less to detect small particles or droplets in the atmosphere. Therefore, CALIPSO instruments are more sensitive to tenuous ice clouds and liquid clouds composed of small particles or droplets, which are invisible to instruments using signals of near-infrared or infrared wavelength to detect clouds. Moreover, the LIDAR signal is attenuated rapidly in optically dense clouds that the infrared or near-infrared signals can easily penetrate (Winker et al., 2010). As a result, the CALIPSO observations of ice water content (IWC) are mostly points at the locations where the temperatures is lower than  $-40^\circ\text{C}$  and the altitude is greater than 6 km poleward to 12 km equatorward, and mostly those without precipitating ice. Given the above considerations, the simulated ice water content (IWC) profiles compared with the CALIPSO observations are referred to as only cloud ice in this section.

The simulated dust load over East Asia at 06 UTC on March 21, 2012 is shown in Figure 89a, in which the dust vast areas from West to East China between 35°N and 45°N, and the orbit of the satellite passed through the area with heavy dust load at around 100°E. Along the satellite orbit, the abundant dust particles were transported to as high as 10 km aloft (Figure 89c). At this time, a high concentration of ~~ice-water-content~~IWC was observed along the satellite of around 10 km between 30°N and 45°N (Figure 89e). The simulation result from CTRL (Figure 89g) shows that the model produces some ice cloud at altitude of 9–10 km between 35°N and 45°N, but with much lower ~~ice-water~~ to the observations. Nevertheless, by ~~applying the GOCART-Thompson microphysics scheme, considering~~ the effect much higher ~~ice-water-content~~IWC at altitude of 9–10 km between 35°N and 45°N (Figure 89i), which is much more observations. The comparison between the simulation results from CTRL and DUST indicates that the high ~~ice-water~~ observed by the satellite between 30°N and 35°N might be unrelated to microphysical processes, but instead due to strong convective motions over South China.

On April 1, 2012, Central to East China was covered by a thick dust plume, and the orbit of the satellite passed ~~through areas with heavy dust load~~ between 25°N and 43°N along 120°E at 18 UTC (Figure 89b). Dust particles were distributed vertically from the surface to over 8 km along the satellite orbit (Figure 89d). A band of high ~~ice-water~~ ~~content~~IWC was observed by the satellite at altitude of 5 km to 10 km between 33°N and 44°N (Figure 89f), which was barely reproduced in the results of the CTRL run without dust. In contrast, the observed band of high ~~ice-water~~ ~~content~~IWC was reproduced by the model in DUST with much more consistent location and magnitude (Figure 89j).

At 18 UTC on April 9, 2012, the satellite was scanning the ~~east coast of China~~ ~~dust source over GD~~, which was covered by a thick dust plume between 35°N and 45°N (Figure 10a), with dust particles lifted up to 10 km above the surface (Figure 940c). High concentration of ~~ice-water-content~~IWC was observed by the satellite at altitude from 5 km to 11 km between 30°N and 45°N (Figure 940e). In this case, the model reproduced the high concentration of ~~ice-water~~ ~~content~~IWC at the observed location in the results from both CTRL and DUST, although the ~~ice-water-content~~IWC was significantly underestimated in the results from CTRL (Figure 940g), while it was ~~well-better~~ reproduced in the results from DUST (Figure 940j).

Similar to the previous cases, the satellite was scanning along east coast of China at 05 UTC on April 23, 2012, when a dust plume was arriving ~~in East China~~ ~~from the dust sources~~ and affecting areas between 35°N and 45°N (Figure 940b), and dust particles were distributed vertically from the surface to 10 km along the scanning track of the satellite



(Figure 940d). Along the orbit of the satellite, two bands with high ~~ice-water-content~~IWC were observed at altitudes 12 km, one is located between 30°N and 37°N, and the other is located between 40°N and 45°N (Figure 940f). In the results from CTRL, the model reproduced the bands of high ~~ice-water-content~~IWC at the correct locations, but with values (Figure 940h); however, upon taking into account the effect of dust in the GOCART-Thompson microphysics scheme, the bands of high ~~ice-water-content~~IWC were well reproduced by the model, with much more consistent By comparing the satellite-observational and simulated vertical profiles of ~~ice-water-content~~IWC during the various dust events, it was demonstrated that ~~the newly implemented GOCART-Thompson microphysics scheme by considering the effects of dust on ice nucleation process, the model~~ reproduces the enhancement of ~~ice-water content~~IWC clouds in the mid- to upper troposphere by taking in to account the effect of dust in the ice nucleation process, which substantially improves the simulation of cloud ice.

### 65.2.3 Mean vertical profiles of ~~ice-water-content~~IWC

The mean profiles of the observed ~~ice-water-content~~IWC, as well as the simulated ~~ice-water-content~~IWC from CTRL and DUST for the four dust events discussed in Section 65.2.2, are shown in Figure 104. Note that the “mean profile” of ~~ice-water-content~~IWC is the average over the available data points for the ~~ice-water-content~~IWC along the orbit of the satellite between 30°N to 45°N for each of the dust events shown in Figures 89 and 940f.

Compared with the results from CTRL, ~~the simulation for the vertical profile of the simulated ice-water-content~~IWC was substantially improved in DUST for each dust event, with the enhancement of the ice nucleation process well captured by the GOCART-Thompson microphysics scheme, ~~although~~ However, there were still discrepancies between observations and the simulation results from DUST, ~~the magnitudes of the vertical IWC produced by the model were always lower than the observed values.~~

For the cases on March 21 and April 1, the peaks of ~~ice-water-content~~IWC were observed at 9.5 km and 8 km, respectively, whereas the simulated peak of ~~ice-water-content~~IWC were located at 8 km and 7.5 km, respectively, with lower peak values. The lower peak value for the case on March 21 was due to the missing of the high ~~ice-water content~~IWC observed between 30°N to 45°N in the simulation results (Figure 89e and i), while the lower peak value for the case on April 1 was due to the underestimation of the ~~ice-water-content~~IWC around 35°N (Figure 89f and j).

The locations of the peaks of simulated ~~ice-water-content~~IWC for the cases on April 9 and April 23 ~~are-were~~ more observed peaks, but still possessed lower values due to the missing or underestimation of high ~~ice-water-content~~IWC the observations.

### 6.5.3 Sensitivity test and discussion

As discussed in Section 6.5.2.3, the simulation of cloud ice is greatly improved by considering the enhancement of ice nucleation process induced by dust, which is well captured by the GOCART–Thompson microphysics scheme. However, the ~~ice-water-content~~IWC is still underestimated by the model during dust events. To determine the reason for this limitation, numerical experiments were performed to investigate the sensitivity of simulated ~~ice-water-content~~IWC to the parameters ~~for-of~~ the ice nucleation parameterization in the GOCART–Thompson microphysics scheme.

#### 6.5.3.1 Calibration factor $c_f$

The calibration factor  $c_f$  is an empirical tuning coefficient derived from observational data from field and laboratory experiments. It ranges from 1 to 6, and recommended to be 3 (DeMott et al., 2015), which was applied in the previous simulations. ~~Three other experiments were~~An experiment was conducted to investigate the sensitivity of the simulated ~~ice-water-content~~IWC to  $c_f$  values ranging from 3 to 6.

The mean profiles of ~~ice-water-content~~IWC from simulation results were compared with the CALIPSO observations for the dust events discussed in Section 6.5.2.2 and 6.5.2.3, as shown in Figure 11.2. For the cases on March 21 and April 1, changing  $c_f$  did not result in an increase of ~~ice-water-content~~IWC; instead, the simulated ~~ice-water-content~~IWC remained consistent for  $c_f$  values varying from 3 to 6. ~~As ice nucleation occurs only in a super-saturated atmosphere with respect to water vapor, an upper limit was set in the Thompson–Eidhammer microphysics scheme, in that once the coagulation-freezing of droplets makes the relative humidity in the atmosphere lower than the threshold relative humidity, which was set to 105% in the simulations, the ice nucleation process is terminated. The consis indicates that the water vapor available for freezing into ice crystals has been consumed up when  $c_f$  was set to 3, therefore,~~

~~increasing  $c_f$  could not lead to an increase in simulated IWC. The consistency in simulated ice water content with~~

For the case on April 9, the simulated ~~ice water content~~IWC increased between 6 km and 9 km and ~~matched was closer~~  
~~ro~~ the observed profile ~~better~~ when  $c_f$  was equal to 4 and 5; however, when  $c_f$  was set to ~~3 and~~ 6, the simulated ~~ice~~  
~~water content~~IWC was lower than that obtained with  $c_f$  values of 4 or 5; ~~although it matched the observed profile~~  
~~better than that produced with a  $c_f$  of 3.~~

For the case on April 23, two peaks were observed in the profile~~s~~ of simulated ~~ice water content~~IWC, located at 7 km  
and 10 km. The simulated ~~ice water content~~IWC remained unchanged with  $c_f$  values varying from 3 to 6 for the peak  
at 10 km, but increased upon changing the  $c_f$  from 3 to 4, and remained the same upon changing the  $c_f$  from 5 and 6  
for the peak ~~at 7 km. In this case,~~ The peak of the simulated ~~ice water content~~IWC at 7 km should correspond to the  
observed peak between 6 km to 8 km, which was slightly overestimated by the model; ~~and increasing the  $c_f$  resulted~~  
~~in even larger overestimation of this peak.~~

~~Given the above discussion~~In summary, increasing the calibration factor  $c_f$  from 3 to 6 does not necessarily lead to a  
significant variation in the simulated ~~ice water content~~IWC during dust events, and the model achieves a relatively  
better performance in reproducing the profile of ~~ice water content~~IWC when the  $c_f$  is set to ~~43~~ or ~~54~~.

~~As ice nucleation occurs only in a super-saturated atmosphere with respect to water vapor, the ice nucleation process~~  
~~would be terminated in the GOCART-Thompson microphysics scheme when the environmental  $RH_i$  is lower than the~~  
~~threshold  $RH_i$ , which was set to 105% for the simulations in this study. The consistency in the simulated IWC with~~  
~~increasing  $c_f$  for the cases in Figure 11 indicates that in these cases, the environmental  $RH_i$  had already reached below~~  
~~105% when  $c_f$  was set to 3, meaning that the water vapor available for freezing into ice crystals has been consumed~~  
~~up with  $c_f$  equal to 3, therefore, increasing  $c_f$  could not lead to a further increase in simulated IWC. Given the above,~~  
~~lowering the threshold  $RH_i$  might result in an enhancement of the ice nucleation process as well as the simulated IWC,~~  
~~which will be discussed in the following section.~~

### 6.3.2 Threshold of relative humidity

In this study, the threshold relative humidity to trigger the ice nucleation process in the simulation was originally set to 105%, which was selected for the central lamina condition in the laboratory experiments to derive the DeMott2015 ice nucleation scheme (DeMott et al., 2015). However, as reported in other studies, the number of ice nucleating particles starts to rise when the relative humidity exceeds 100% (DeMott et al., 2011). Therefore, a sensitivity experiment was carried out to investigate the response of simulated ~~ice-water-content~~IWC to lower threshold relative humidity.

The mean profiles of ~~ice-water-content~~IWC from the simulation results were compared with ~~the~~ CALIPSO observations for the aforementioned dust events, as shown in Figure 1 ~~23~~. With the threshold relative humidity lowered to 100%, the simulated ~~ice-water-content~~IWC showed an increase throughout the vertical profile, with the most significant increase at the peaks, suggesting more consistency with the observations for all of the dust events, except the one on April 1. In the case on April 1, the simulated ~~ice-water-content~~IWC increased at lower ~~layers-altitudes~~ than the observed peak, but slightly decreased right at the peak upon-with lowering the threshold relative humidity to 100% ~~for the ease~~. Overall, the simulation of ~~ice-water-content~~IWC during dust events was significantly improved by lowering the threshold relative humidity from 105% to 100%.

## 76 Conclusions

A new ~~microphysics-scheme~~treatment, the GOCART–Thompson scheme, ~~has been was~~ implemented into WRF-Chem to couple the GOCART ~~aerosol~~dust model ~~to and~~ the aerosol-aware Thompson-~~Eidhammer~~ microphysics scheme. By applying this newly-implemented microphysics scheme, the effect of dust on the ice nucleation process by serving as ~~ice-nuclei~~IN in the atmosphere can be quantified and evaluated ~~by the model simultaneously with dust simulation~~. Numerical experiments, including a control run without dust and a test run with dust, were then carried out to evaluate the performance of the newly-implemented GOCART–Thompson microphysics scheme in simulating the effect of dust on the content of cloud ice over East Asia during a typical dust-intensive period, by comparing the simulation results with various observations.

Based on the GOCART aerosol model the model reproduce~~s~~ dust emission reasonably well, by capturing the ~~trend~~ evolution and magnitude of surface PM<sub>10</sub> concentration at the locations of various environmental monitoring stations

627 and the AOD at two AERONET sites. The spatial patterns of the mean AOD over East Asia during the simulation  
628 period were also consistent with satellite observations.

629 The effect of dust on the ice nucleation process ~~by serving as ice nuclei~~ was then quantified and evaluated in the  
630 GOCART–Thompson microphysics scheme. Upon considering the effect of dust in the simulation, the simulated ice  
631 water mixing ratio and ice crystal number concentration over East Asia were one order of magnitude higher than those  
632 simulated without dust, with the most significant enhancements located over dust source regions and downwind areas.

633 By comparing the ~~mean~~-simulated ~~ice-water-path~~IWP ~~averaged~~ over East Asia during the simulation period with  
634 MODIS observations, it was demonstrated that the ~~ice-water-path~~IWP including cloud ice and precipitating ice ~~was~~  
635 reasonably reproduced by the model over most areas of East Asia, ~~although slightly underestimated, with~~ The results  
636 from the simulation run with dust ~~were~~ more consistent with the observations.

637 Comparison between the vertical profiles of the satellite-observed and simulated ~~ice-water-content~~IWC during various  
638 dust events ~~and the entire simulation period further~~ indicated that the enhancement of cloud ice induced by abundant  
639 dust particles serving as ~~ice nuclei~~IN is well captured by the GOCART–Thompson microphysics scheme, with the  
640 results from the simulation with dust much more consistent with the satellite–observations, ~~although the IWC is~~  
641 ~~generally underestimated by the model.~~

642 Sensitivity experiments revealed that the simulated ~~ice-water-content~~IWC ~~was~~ not very sensitive to the calibration  
643 factor ~~defined~~ in the DeMott2015 ice nucleation scheme, but the model delivered a slight better performance in  
644 reproducing the ~~ice-water-content~~IWC when the calibration factor was set to 3 or 4. However, the simulated ~~ice-water~~  
645 ~~content~~IWC ~~was~~ sensitive to the threshold relative humidity to trigger the ice nucleation process in the model, ~~and~~  
646 ~~the simulation of ice-water-content~~and ~~was~~ significantly improved upon lowering the threshold relative humidity  
647 from 105% to 100%.

648

649 **Acknowledgement.** We would like to acknowledge the provision of the MODIS and the MISR observations by the  
650 Ministry of Environmental Protection Data Center, U.S. National Center for Atmospheric Research (NCAR), and the  
651 CALIPSO data by the U.S. National Aeronautics and Space Administration (NASA) Data Center. We thank the  
652 principal investigators and their staff for establishing and maintaining the two AERONET sites used in this study. The

653 AERONET data were obtained freely from the AERONET program website (<https://aeronet.gsfc.nasa.gov/>). We  
654 appreciate the assistance of the Hong Kong Observatory (HKO), which provided the meteorological data. Lin Su  
655 would like to thank Dr. Georg Grell, Dr. Stuart McKeen, and Dr. Ravan Ahmandov from the Earth System Research  
656 Laboratory, U.S. National Oceanic and Atmospheric Administration for insightful discussions. Other data used this  
657 paper are properly cited and referred to in the reference list. All data shown in the results are available upon request.  
658 This work was supported by NSFC/RGC Grant N\_HKUST631/05,  
659 NSFC-FD Grant U1033001, and the RGC Grant 16303416.

660

## 661    **References**

- 662    Atkinson, J. D., Murray, B. J., Woodhouse, M. T., Whale, T. F., Baustian, K. J., Carslaw, K. S., Dobbie, S., O'sullivan,  
663    D., and Malkin, T. L.: The importance of feldspar for ice nucleation by mineral dust in mixed-phase clouds, *Nature*,  
664    498, 355, 2013.
- 665    Baró, R., Jiménez-Guerrero, P., Balzarini, A., Curci, G., Forkel, R., Grell, G., Hirtl, M., Honzak, L., Langer, M., and  
666    Pérez, J. L.: Sensitivity analysis of the microphysics scheme in WRF-Chem contributions to AQMEII phase 2,  
667    *Atmospheric Environment*, 115, 620-629, 2015.
- 668    Bi, J., Huang, J., Fu, Q., Ge, J., Shi, J., Zhou, T., and Zhang, W.: Field measurement of clear-sky solar irradiance in  
669    Badain Jaran Desert of Northwestern China, *Journal of Quantitative Spectroscopy and Radiative Transfer*, 122, 194-  
670    207, 2013.
- 671    Chapman, E. G., Gustafson Jr, W., Easter, R. C., Barnard, J. C., Ghan, S. J., Pekour, M. S., and Fast, J. D.: Coupling  
672    aerosol-cloud-radiative processes in the WRF-Chem model: Investigating the radiative impact of elevated point  
673    sources, *Atmospheric Chemistry and Physics*, 9, 945-964, 2009.
- 674    Chin, M., Rood, R. B., Lin, S.-J., Müller, J.-F., and Thompson, A. M.: Atmospheric sulfur cycle simulated in the  
675    global model GOCART: Model description and global properties, 2000.
- 676    DeMott, P. J., Sassen, K., Poellot, M. R., Baumgardner, D., Rogers, D. C., Brooks, S. D., Prenni, A. J., and  
677    Kreidenweis, S. M.: African dust aerosols as atmospheric ice nuclei, *Geophysical Research Letters*, 30, 2003.
- 678    DeMott, P. J., Prenni, A. J., Liu, X., Kreidenweis, S. M., Petters, M. D., Twohy, C. H., Richardson, M., Eidhammer,  
679    T., and Rogers, D.: Predicting global atmospheric ice nuclei distributions and their impacts on climate, *Proceedings*  
680    *of the National Academy of Sciences*, 107, 11217-11222, 2010.
- 681    DeMott, P. J., Möhler, O., Stetzer, O., Vali, G., Levin, Z., Petters, M. D., Murakami, M., Leisner, T., Bundke, U., and  
682    Klein, H.: Resurgence in ice nuclei measurement research, *Bulletin of the American Meteorological Society*, 92, 1623-  
683    1635, 2011.
- 684    DeMott, P. J., Prenni, A. J., McMeeking, G. R., Sullivan, R. C., Petters, M. D., Tobo, Y., Niemand, M., Möhler, O.,  
685    Snider, J. R., and Wang, Z.: Integrating laboratory and field data to quantify the immersion freezing ice nucleation  
686    activity of mineral dust particles, *Atmospheric Chemistry and Physics*, 15, 393-409, 2015.
- 687    Diner, D. J., Barge, L. M., Bruegge, C. J., Chrien, T. G., Conel, J. E., Eastwood, M. L., Garcia, J. D., Hernandez, M.  
688    A., Kurzweil, C. G., and Ledebor, W. C.: The Airborne Multi-angle Imaging SpectroRadiometer (AirMISR):  
689    instrument description and first results, *IEEE Transactions on Geoscience and Remote Sensing*, 36, 1339-1349, 1998.
- 690    Duce, R., Liss, P., Merrill, J., Atlas, E., Buat-Menard, P., Hicks, B., Miller, J., Prospero, J., Arimoto, R., and Church,  
691    T.: The atmospheric input of trace species to the world ocean, *Global biogeochemical cycles*, 5, 193-259, 1991.
- 692    Ge, J., Su, J., Ackerman, T., Fu, Q., Huang, J., and Shi, J.: Dust aerosol optical properties retrieval and radiative  
693    forcing over northwestern China during the 2008 China-US joint field experiment, *Journal of Geophysical Research:*  
694    *Atmospheres*, 115, 2010.
- 695    Ginoux, P., Chin, M., Tegen, I., Prospero, J. M., Holben, B., Dubovik, O., and Lin, S. J.: Sources and distributions of  
696    dust aerosols simulated with the GOCART model, *Journal of Geophysical Research: Atmospheres*, 106, 20255-20273,  
697    2001.

698 Ginoux, P., Prospero, J. M., Torres, O., and Chin, M.: Long-term simulation of global dust distribution with the  
 699 GOCART model: correlation with North Atlantic Oscillation, *Environmental Modelling & Software*, 19, 113-128,  
 700 2004.  
 701 Grell, G., Peckham, S., Fast, J., Singh, B., Easter, R., Gustafson, W., Rasch, P., Wolters, S., Barth, M., and Pfister, G.:  
 702 WRF-Chem V3. 5: A summary of status and updates, *EGU General Assembly Conference Abstracts*, 2013, 11332.  
 703 Grell, G. A., and Freitas, S. R.: A scale and aerosol aware stochastic convective parameterization for weather and air  
 704 quality modeling, *Atmos. Chem. Phys.*, 14, 5233-5250, 2014.  
 705 Hansen, J., Sato, M., and Ruedy, R.: Radiative forcing and climate response, *Journal of Geophysical Research:*  
 706 *Atmospheres*, 102, 6831-6864, 1997.  
 707 Hartmann, D., Tank, A., and Rusticucci, M.: IPCC fifth assessment report, climate change 2013: The physical science  
 708 basis, *IPCC AR5*, 31-39, 2013.  
 709 Holben, B., Tanre, D., Smirnov, A., Eck, T., Slutsker, I., Abuhassan, N., Newcomb, W., Schafer, J., Chatenet, B., and  
 710 Lavenue, F.: An emerging ground-based aerosol climatology: Aerosol optical depth from AERONET, *Journal of*  
 711 *Geophysical Research: Atmospheres*, 106, 12067-12097, 2001.  
 712 Hoose, C., Lohmann, U., Erdin, R., and Tegen, I.: The global influence of dust mineralogical composition on  
 713 heterogeneous ice nucleation in mixed-phase clouds, *Environmental Research Letters*, 3, 025003, 2008.  
 714 Horvath, H.: Influence of atmospheric aerosols upon the global radiation balance, *Atmospheric particles*, 5, 62-63,  
 715 1998.  
 716 Hsu, N. C., Tsay, S.-C., King, M. D., and Herman, J. R.: Deep blue retrievals of Asian aerosol properties during ACE-  
 717 Asia, *IEEE Transactions on Geoscience and Remote Sensing*, 44, 3180-3195, 2006.  
 718 Hsu, S. C., Liu, S. C., Arimoto, R., Liu, T. H., Huang, Y. T., Tsai, F., Lin, F. J., and Kao, S. J.: Dust deposition to the  
 719 East China Sea and its biogeochemical implications, *Journal of Geophysical Research: Atmospheres*, 114, 2009.  
 720 Huang, J., Fu, Q., Su, J., Tang, Q., Minnis, P., Hu, Y., Yi, Y., and Zhao, Q.: Taklimakan dust aerosol radiative heating  
 721 derived from CALIPSO observations using the Fu-Liou radiation model with CERES constraints, *Atmospheric*  
 722 *Chemistry and Physics*, 9, 4011-4021, 2009.  
 723 Huang, J.: Emission, transport, and radiative effects of mineral dust from the Taklimakan and Gobi deserts:  
 724 comparison of measurements and model results, *Atmos. Chem. Phys.*, 1680, 7324, 2017.  
 725 Iacono, M. J., Delamere, J. S., Mlawer, E. J., Shephard, M. W., Clough, S. A., and Collins, W. D.: Radiative forcing  
 726 by long-lived greenhouse gases: Calculations with the AER radiative transfer models, *Journal of Geophysical*  
 727 *Research: Atmospheres*, 113, 2008.  
 728 Janjić, Z. I.: The step-mountain eta coordinate model: Further developments of the convection, viscous sublayer, and  
 729 turbulence closure schemes, *Monthly Weather Review*, 122, 927-945, 1994.  
 730 Janjić, Z. I.: Nonsingular implementation of the Mellor–Yamada level 2.5 scheme in the NCEP Meso model, *NCEP*  
 731 *office note*, 437, 61, 2002.  
 732 Kang, J. Y., Yoon, S. C., Shao, Y., and Kim, S. W.: Comparison of vertical dust flux by implementing three dust  
 733 emission schemes in WRF/Chem, *Journal of Geophysical Research: Atmospheres*, 116, 2011.



734 Karydis, V., Kumar, P., Barahona, D., Sokolik, I., and Nenes, A.: On the effect of dust particles on global cloud  
 735 condensation nuclei and cloud droplet number, *Journal of Geophysical Research: Atmospheres*, 116, 2011.  
 736 Kaufman, Y., Tanré, D., Remer, L. A., Vermote, E., Chu, A., and Holben, B.: Operational remote sensing of  
 737 tropospheric aerosol over land from EOS moderate resolution imaging spectroradiometer, *Journal of Geophysical*  
 738 *Research: Atmospheres*, 102, 17051-17067, 1997.  
 739 Koehler, K., Kreidenweis, S., DeMott, P., Petters, M., Prenni, A., and Möhler, O.: Laboratory investigations of the  
 740 impact of mineral dust aerosol on cold cloud formation, *Atmospheric Chemistry and Physics*, 10, 11955-11968, 2010.  
 741 Koop, T., Luo, B., Tsias, A., and Peter, T.: Water activity as the determinant for homogeneous ice nucleation in  
 742 aqueous solutions, *Nature*, 406, 611-614, 2000.  
 743 Lacis, A.: Climate forcing, climate sensitivity, and climate response: A radiative modeling perspective on atmospheric  
 744 aerosols, *Aerosol forcing of climate*, 11-42, 1995.  
 745 Liu, Huang, J., Shi, G., Takamura, T., Khatri, P., Bi, J., Shi, J., Wang, T., Wang, X., and Zhang, B.: Aerosol optical  
 746 properties and radiative effect determined from sky-radiometer over Loess Plateau of Northwest China, *Atmospheric*  
 747 *Chemistry and Physics*, 11, 11455-11463, 2011a.  
 748 Liu, Zheng, Y., Li, Z., Flynn, C., Welton, E. J., and Cribb, M.: Transport, vertical structure and radiative properties of  
 749 dust events in southeast China determined from ground and space sensors, *Atmospheric environment*, 45, 6469-6480,  
 750 2011b.  
 751 Lohmann, U., and Diehl, K.: Sensitivity studies of the importance of dust ice nuclei for the indirect aerosol effect on  
 752 stratiform mixed-phase clouds, *Journal of the Atmospheric Sciences*, 63, 968-982, 2006.  
 753 Mallet, M., Tulet, P., Serça, D., Solmon, F., Dubovik, O., Pelon, J., Pont, V., and Thouaron, O.: Impact of dust aerosols  
 754 on the radiative budget, surface heat fluxes, heating rate profiles and convective activity over West Africa during  
 755 March 2006, *Atmospheric Chemistry and Physics*, 9, 7143-7160, 2009.  
 756 Martonchik, J., Diner, D., Kahn, R., Gaitley, B., and Holben, B.: Comparison of MISR and AERONET aerosol optical  
 757 depths over desert sites, *Geophysical Research Letters*, 31, 2004.  
 758 Miller, R., Tegen, I., and Perlwitz, J.: Surface radiative forcing by soil dust aerosols and the hydrologic cycle, *Journal*  
 759 *of Geophysical Research: Atmospheres*, 109, 2004.  
 760 Mlawer, E. J., Taubman, S. J., Brown, P. D., Iacono, M. J., and Clough, S. A.: Radiative transfer for inhomogeneous  
 761 atmospheres: RRTM, a validated correlated-k model for the longwave, *Journal of Geophysical Research: Atmospheres*,  
 762 102, 16663-16682, 1997.  
 763 Nabat, P., Somot, S., Mallet, M., Michou, M., Sevault, F., Driouech, F., Meloni, D., Di Sarra, A., Di Biagio, C., and  
 764 Formenti, P.: Dust aerosol radiative effects during summer 2012 simulated with a coupled regional aerosol–  
 765 atmosphere–ocean model over the Mediterranean, *Atmospheric Chemistry and Physics*, 15, 3303-3326, 2015a.  
 766 Nabat, P., Somot, S., Mallet, M., Sevault, F., Chiacchio, M., and Wild, M.: Direct and semi-direct aerosol radiative  
 767 effect on the Mediterranean climate variability using a coupled regional climate system model, *Climate dynamics*, 44,  
 768 1127-1155, 2015b.  
 769 Perlwitz, J., and Miller, R. L.: Cloud cover increase with increasing aerosol absorptivity: A counterexample to the  
 770 conventional semidirect aerosol effect, *Journal of Geophysical Research: Atmospheres*, 115, 2010.

771 Phillips, V. T., DeMott, P. J., and Andronache, C.: An empirical parameterization of heterogeneous ice nucleation for  
 772 multiple chemical species of aerosol, *Journal of the atmospheric sciences*, 65, 2757-2783, 2008.  
 773 Seigel, R., Van Den Heever, S., and Saleeby, S.: Mineral dust indirect effects and cloud radiative feedbacks of a  
 774 simulated idealized nocturnal squall line, *Atmospheric Chemistry and Physics*, 13, 4467-4485, 2013.  
 775 Shao: A model for mineral dust emission, *Journal of Geophysical Research: Atmospheres*, 106, 20239-20254, 2001.  
 776 Shao: Simplification of a dust emission scheme and comparison with data, *Journal of Geophysical Research:*  
 777 *Atmospheres*, 109, 2004.  
 778 Shao, Ishizuka, M., Mikami, M., and Leys, J.: Parameterization of size-resolved dust emission and validation with  
 779 measurements, *Journal of Geophysical Research: Atmospheres*, 116, 2011.  
 780 Soil Survey Staff: Soil survey manual, 1993.  
 781 Solomos, S., Kallos, G., Kushta, J., Astitha, M., Tremback, C., Nenes, A., and Levin, Z.: An integrated modeling  
 782 study on the effects of mineral dust and sea salt particles on clouds and precipitation, *Atmospheric Chemistry and*  
 783 *Physics*, 11, 873-892, 2011.  
 784 Su, L., and Fung, J. C.: Sensitivities of WRF-Chem to dust emission schemes and land surface properties in simulating  
 785 dust cycles during springtime over East Asia, *Journal of Geophysical Research: Atmospheres*, 120, 2015.  
 786 Tesfaye, M., Tsidu, G. M., Botai, J., and Sivakumar, V.: Mineral dust aerosol distributions, its direct and semi-direct  
 787 effects over South Africa based on regional climate model simulation, *Journal of Arid Environments*, 114, 22-40,  
 788 2015.  
 789 Textor, C., Schulz, M., Guibert, S., Kinne, S., Balkanski, Y., Bauer, S., Berntsen, T., Berglen, T., Boucher, O., and  
 790 Chin, M.: Analysis and quantification of the diversities of aerosol life cycles within AeroCom, *Atmospheric Chemistry*  
 791 *and Physics*, 6, 1777-1813, 2006.  
 792 Thompson, G., Rasmussen, R. M., and Manning, K.: Explicit forecasts of winter precipitation using an improved bulk  
 793 microphysics scheme. Part I: Description and sensitivity analysis, *Monthly Weather Review*, 132, 519-542, 2004.  
 794 Thompson, G., and Eidhammer, T.: A study of aerosol impacts on clouds and precipitation development in a large  
 795 winter cyclone, *Journal of the Atmospheric Sciences*, 71, 3636-3658, 2014.  
 796 Tomasi, C., Fuzzi, S., and Kokhanovsky, A.: *Atmospheric Aerosols: Life Cycles and Effects on Air Quality and*  
 797 *Climate*, John Wiley & Sons, 2017.  
 798 Twohy, C. H., Kreidenweis, S. M., Eidhammer, T., Browell, E. V., Heymsfield, A. J., Bansemer, A. R., Anderson, B.  
 799 E., Chen, G., Ismail, S., and DeMott, P. J.: Saharan dust particles nucleate droplets in eastern Atlantic clouds,  
 800 *Geophysical Research Letters*, 36, 2009.  
 801 Vaughan, M. A., Young, S. A., Winker, D. M., Powell, K. A., Omar, A. H., Liu, Z., Hu, Y., and Hostetler, C. A.: Fully  
 802 automated analysis of space-based lidar data: An overview of the CALIPSO retrieval algorithms and data products,  
 803 *Remote Sensing*, 2004, 16-30.  
 804 Wesely, M.: Parameterization of surface resistances to gaseous dry deposition in regional-scale numerical models,  
 805 *Atmospheric Environment* (1967), 23, 1293-1304, 1989.

806 Winker, Pelon, J., Coakley Jr, J., Ackerman, S., Charlson, R., Colarco, P., Flamant, P., Fu, Q., Hoff, R., and Kittaka,  
807 C.: The CALIPSO mission: A global 3D view of aerosols and clouds, *Bulletin of the American Meteorological Society*,  
808 91, 1211-1229, 2010.

809 Winker, D. M., Vaughan, M. A., Omar, A., Hu, Y., Powell, K. A., Liu, Z., Hunt, W. H., and Young, S. A.: Overview  
810 of the CALIPSO mission and CALIOP data processing algorithms, *Journal of Atmospheric and Oceanic Technology*,  
811 26, 2310-2323, 2009.

812 Zhang, C., Wang, M., Morrison, H., Somerville, R. C., Zhang, K., Liu, X., and Li, J. L. F.: Investigating ice nucleation  
813 in cirrus clouds with an aerosol-enabled Multiscale Modeling Framework, *Journal of Advances in Modeling Earth*  
814 *Systems*, 6, 998-1015, 2014.

815

816

817 **List of tables and figures**

818 [Table 1: Performance statistics for the model in simulating surface PM<sub>10</sub> concentrations at environmental monitoring](#)  
819 [stations during the simulation period.](#)~~Table 1: Performance statistics for the model in simulating surface PM<sub>10</sub>~~  
820 ~~concentrations at environmental monitoring stations during the simulation period.~~

821 [Figure 1: Nested domain set for the simulations. Blue dots represent the ten monitoring stations used for model](#)  
822 [validation. TD: the Taklimakan Desert; GD: The Gobi Desert.](#)~~Figure 1: Nested domain set for the simulations. Blue~~  
823 ~~dots represent the weather stations used for model validation. TD: the Taklimakan Desert; GD: The Gobi Desert.~~

824 [Figure 2: Time series of spatially averaged daily dust mass load \(a\) and daily number density of dust particles \(b\) over](#)  
825 [East Asia \(domain 1\) during the simulation period.](#)~~Figure 2: Time series of spatially averaged daily dust mass load (a)~~  
826 ~~and daily number density of ice-friendly aerosol (b) over East Asia (domain 1) during the simulation period.~~

827 [Figure 3: Time series of hourly observed and simulated surface PM<sub>10</sub> concentrations at various environmental](#)  
828 [monitoring stations. r represents the correlation coefficient between simulation results and observations.](#)~~Figure 3:~~  
829 ~~Time series of hourly observed and simulated surface PM<sub>10</sub> concentrations at various environmental monitoring~~  
830 ~~stations.~~

831 [Figure 4: Time series of daily mean observed and simulated aerosol optical depths at Dalanzadgad \(a\) and SACOL](#)  
832 [\(b\). r represents the correlation coefficient between simulation results and observations.](#)~~Figure 4: Time series of daily~~  
833 ~~mean observed and simulated aerosol optical depths at Dalanzadgad (a) and SACOL (b).~~

834 [Figure 5: Spatial distributions of monthly mean AOD from MODIS observations \(a, b\), MISR observations \(c, d\), and](#)  
835 [simulation results \(e, f\) for March \(left panel\) and April \(right panel\) of 2012.](#)~~Figure 5: Spatial distributions of monthly~~  
836 ~~mean AOD from MODIS observations (a, b), MISR observations (c, d), and simulation results (e, f) for March (left~~  
837 ~~panel) and April (right panel) of 2012.~~

838 [Figure 6: Simulated cloud ice mixing ratio \(a\) and cloud ice crystal number concentration \(b\) at each data point from](#)  
839 [CTRL and DUST.](#)~~Figure 6: Simulated cloud ice mixing ratio (a) and cloud ice crystal number concentration (b) at~~  
840 ~~each data point from CTRL and DUST.~~

841 [Figure 7: Spatial distributions for the temporal mean simulated cloud ice water path \(a-c\) and ice crystal number](#)  
842 [density \(d-f\) from CTRL \(left panel\), DUST \(middle panel\), and the difference between CTRL and DUST \(right panel\)](#)  
843 [over East Asia \(domain 1\) during the simulation period.](#)~~Figure 7: Spatial distributions for the temporal mean simulated~~

cloud-ice water path (a-c) and ice-crystal number density (d-f) from CTRL (left panel), DUST (middle panel), and the difference between CTRL and DUST (right panel) over East Asia (domain 1) during the simulation period.

Figure 8: Spatial distribution for simulated dust load and satellite scanning track (a, b); the simulated vertical profile of ice-friendly aerosol (GNIFA) number concentration (c, d), with the orography represented by the shaded area; the CALIPSO vertical profile of IWC (e, f); and the simulated vertical profile of IWC from CTRL (g, h) and DUST (i, j) for the case on March 21 (left panel) and April 1 (right panel) of 2012. Figure 8: Spatial distribution for the mean-ice water path (a) from MODIS observations, and the simulation results of CTRL (b) and DUST (c) during the simulation period.

Figure 9: As Figure 8 but for the cases on April 9 (left panel) and April 23, (right panel) of 2012.

Figure 10: Vertical profiles for the mean observed IWC from CALIPSO, and the simulated IWC from CTRL and DUST for dust events on March 21, April 1, April 9, and April 23, 2012. Figure 9: Spatial distribution for simulated dust load and satellite scanning track (a, b), the simulated vertical profile of ice-friendly aerosol (GNIFA) number concentration (c, d), the CALIPSO vertical profile of ice water content IWC (e, f), and the simulated vertical profile of ice water content IWC from CTRL (g, h) and DUST (i, j) for the case on March 21 (left panel) and April 1 (right panel) of 2012.

Figure 11: Vertical profiles for the mean observed IWC from CALIPSO, and the simulated IWC with various  $c_f$  for the dust events on March 21, April 1, April 9, and April 23, 2012. Figure 12: Vertical profiles for the mean-observed ice water content IWC from CALIPSO, and the simulated ice water content IWC with various  $c_f$  for the dust events on March 21, April 1, April 9, and April 23, 2012.

Figure 12: Vertical profiles for the mean observational IWC from CALIPSO, and the simulated IWC with threshold RH values of 105% and 100% for the dust events on March 21, April 1, April 9, and April 23, 2012. Figure 13: Vertical profiles for the mean-observational ice water content IWC from CALIPSO, and the simulated ice water content IWC with threshold RH values of 105% and 100% for the dust events on March 21, April 1, April 9, and April 23, 2012.

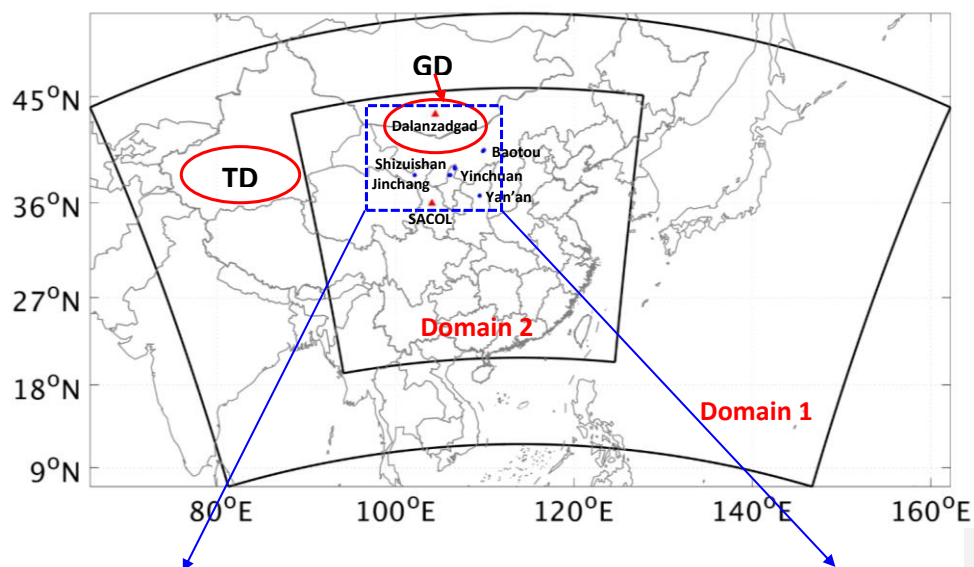
Formatted: Font: Not Bold

**Table 1:** Performance statistics for the model in simulating surface PM<sub>10</sub> concentrations at environmental monitoring stations during the simulation period.

City	STATION NO.	MB (µg/m <sup>3</sup> )	ME (µg/m <sup>3</sup> )	RMSE (µg/m <sup>3</sup> )	r
BAOTOU	XCNAQ77	-36.18	80.43	94.88	0.59
	XCNAQ79	-10.05	75.83	106.58	0.62
SHIZUISHAN	XCNAQ346	72.46	121.18	317.73	0.79
	XCNAQ347	17.64	147.95	294.71	0.75
JINCHANG	XCNAQ340	-108.73	109.09	128.56	0.77
	XCNAQ342	-18.65	46.07	64.78	0.70

YAN'AN	XCNAQ335	-38.93	99.05	149.44	0.68
	XCNAQ336	-60.15	124.74	166.89	0.60
YINCHUAN	XCNAQ344	33.97	112.26	240.27	0.87
	CN_1487	-39.62	155.83	249.00	0.62
Average		-18.84	107.24	181.28	0.70

MB: mean bias; ME: mean error; RMSE: root mean squared error; r: correlation coefficient.



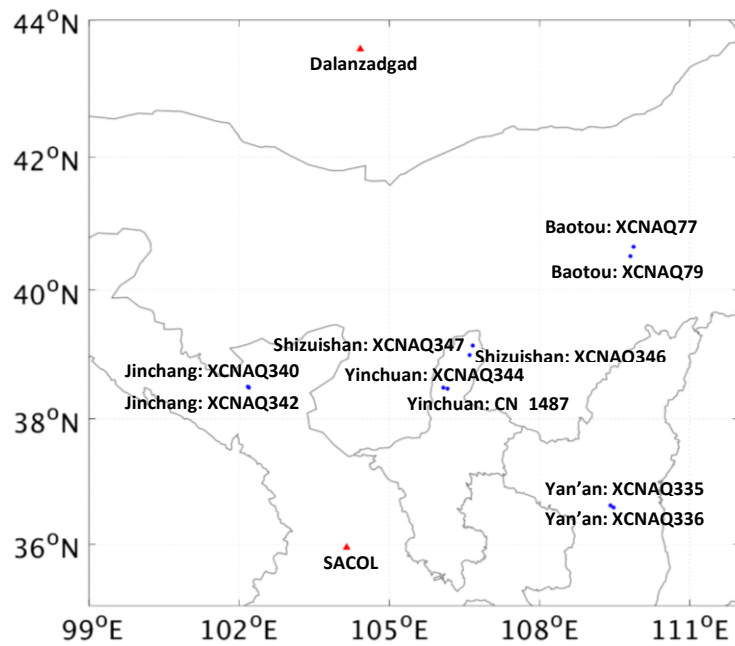


**Figure 1:** Nested domain set for the simulations. Blue dots represent the ten monitoring stations used for model validation. TD: the Taklimakan Desert; GD: The Gobi Desert.

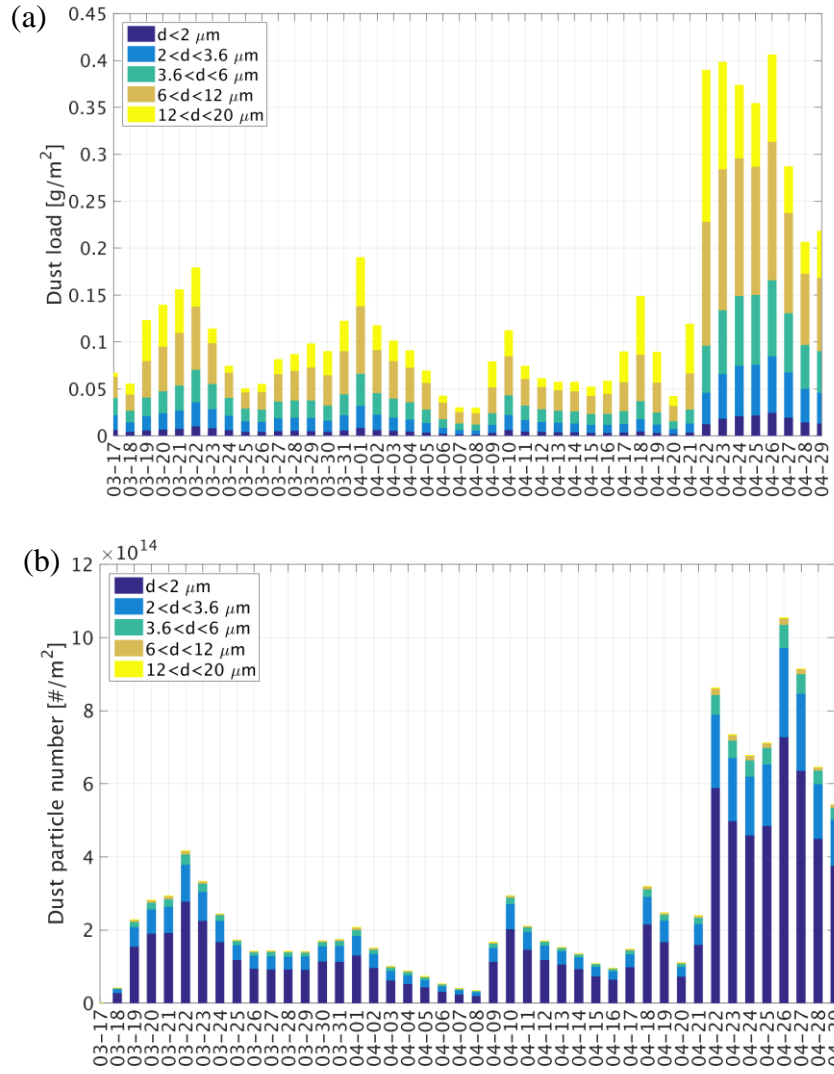


**Figure 2:** Time series of spatially averaged daily dust mass load (a) and daily number density of ice-friendly over East Asia (domain 1) during the simulation period.



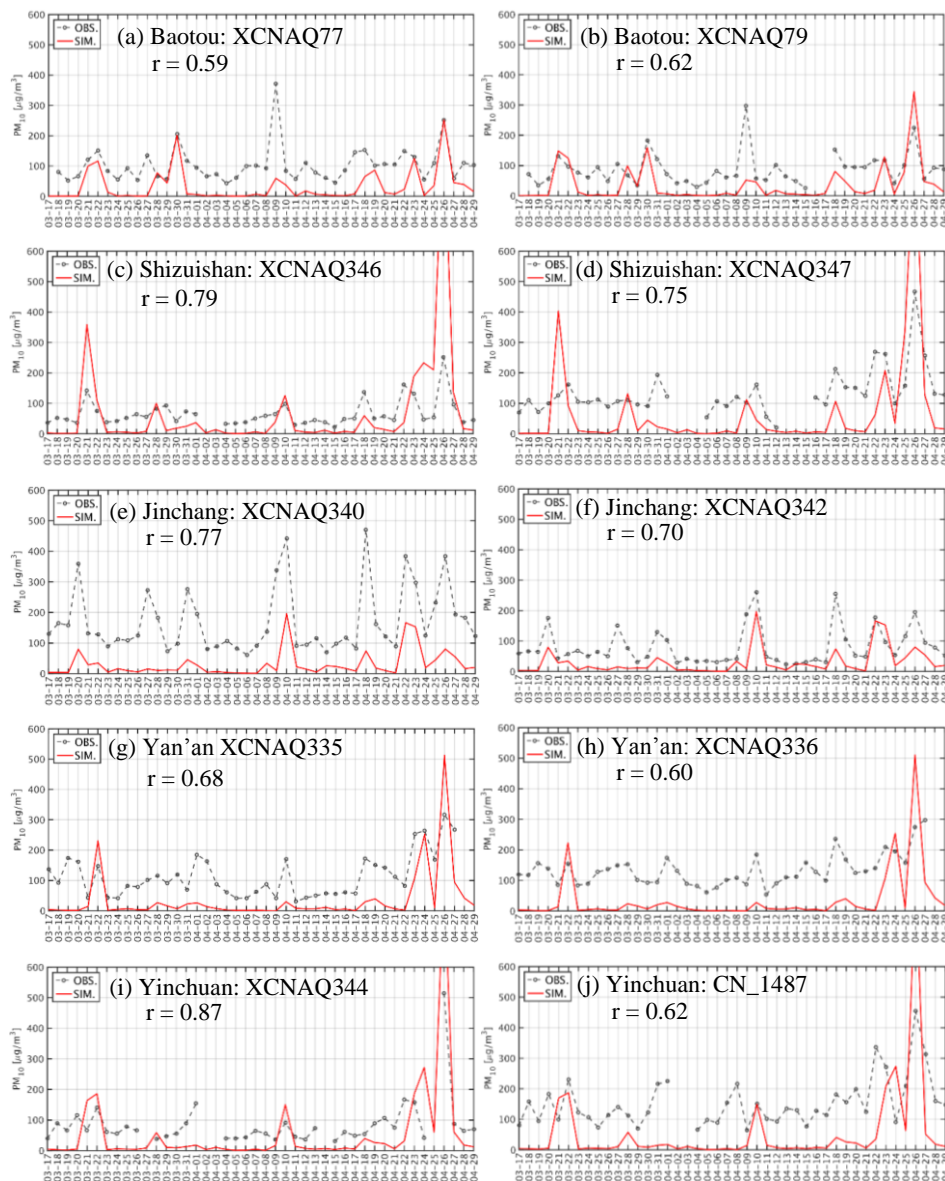


**Figure 3:** Time series of hourly observed and simulated surface  $PM_{10}$  concentrations at various environmental monitoring stations.  $r$  represents the correlation coefficient between simulation results and observations.

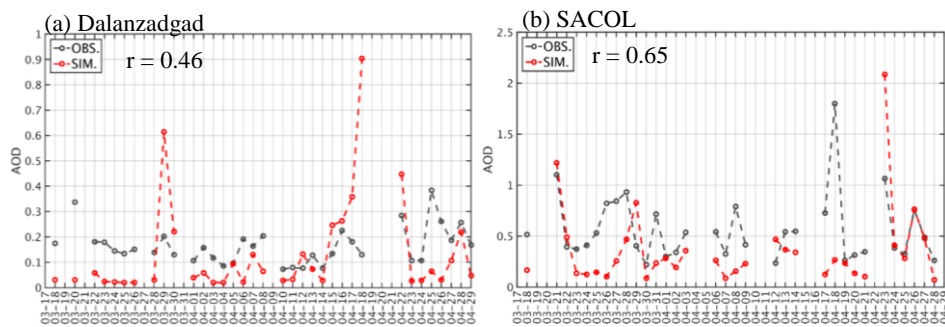


**Figure 4:** Time series of daily mean observed and simulated aerosol optical depths at Dalanzadgad (a) and SACOL (b).  $r$  represents the correlation coefficient between simulation results and observations.

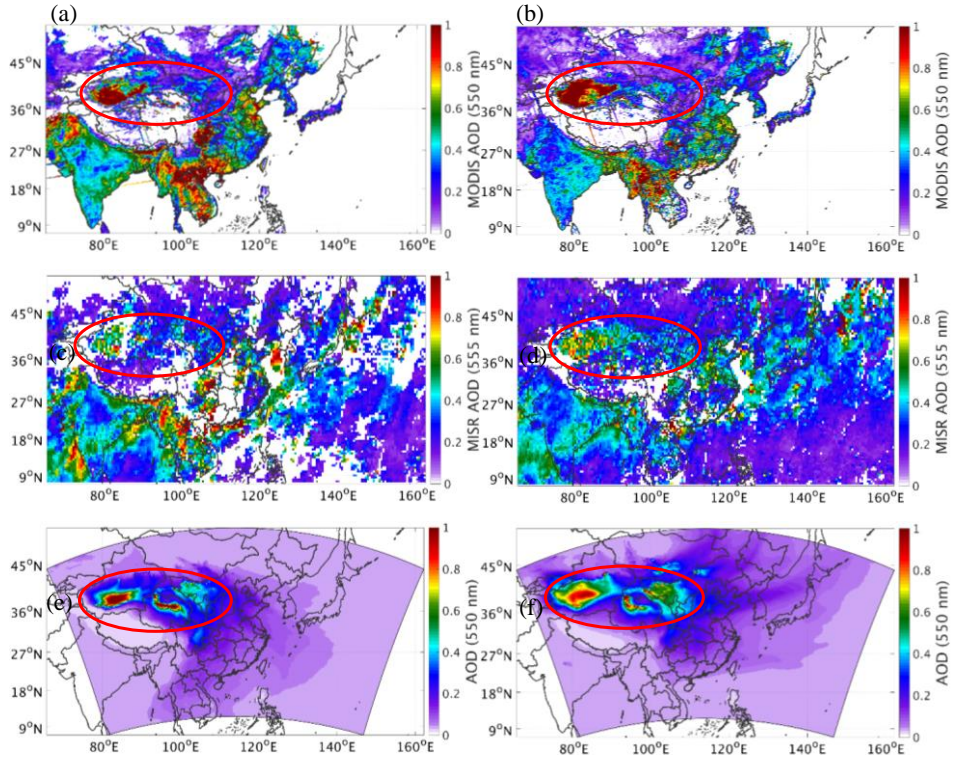


**Figure 5:** Spatial distributions of monthly mean AOD from MODIS observations (a, b), MISR observations (c, d), and simulation results (e, f) for March (left panel) and April (right panel) of 2012.

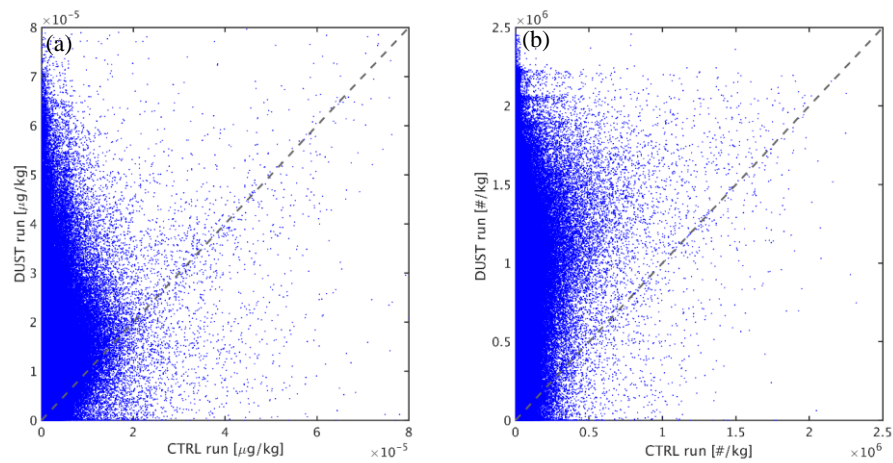


**Figure 6:** Simulated cloud ice mixing ratio (a) and cloud ice crystal number concentration (b) at each data point from CTRL and DUST.

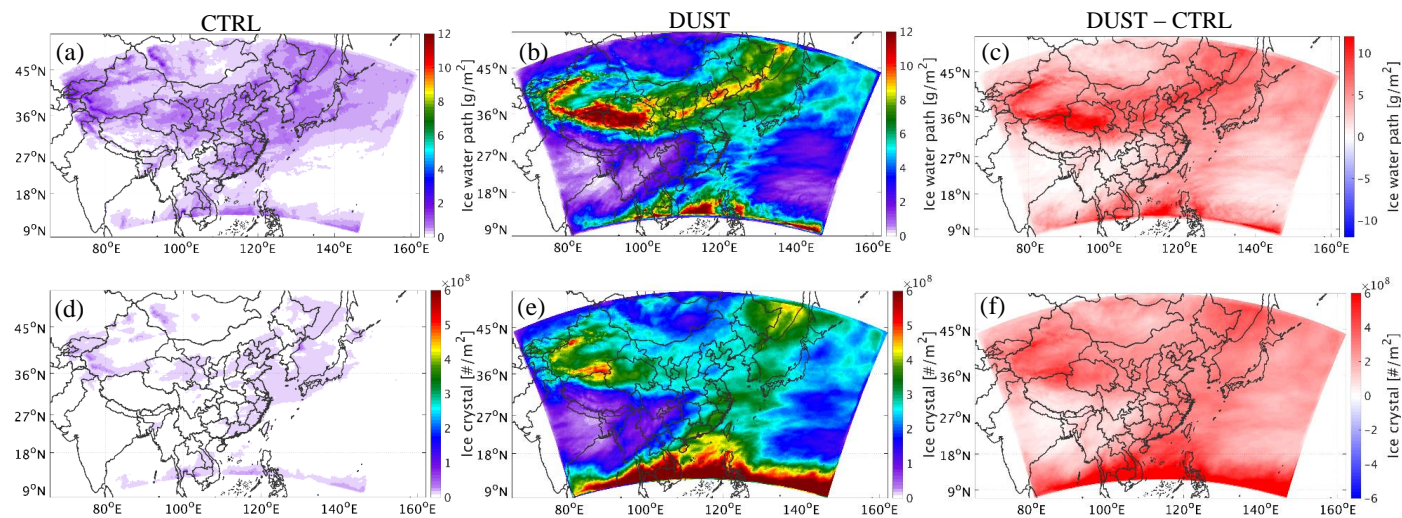


**Figure 7:** Spatial distributions for the temporal mean simulated cloud ice water path (a-c) and ice crystal number density (d-f) from CTRL (left panel), DUST (middle panel), and the difference between CTRL and DUST (right panel) over East Asia (domain 1) during the simulation period.

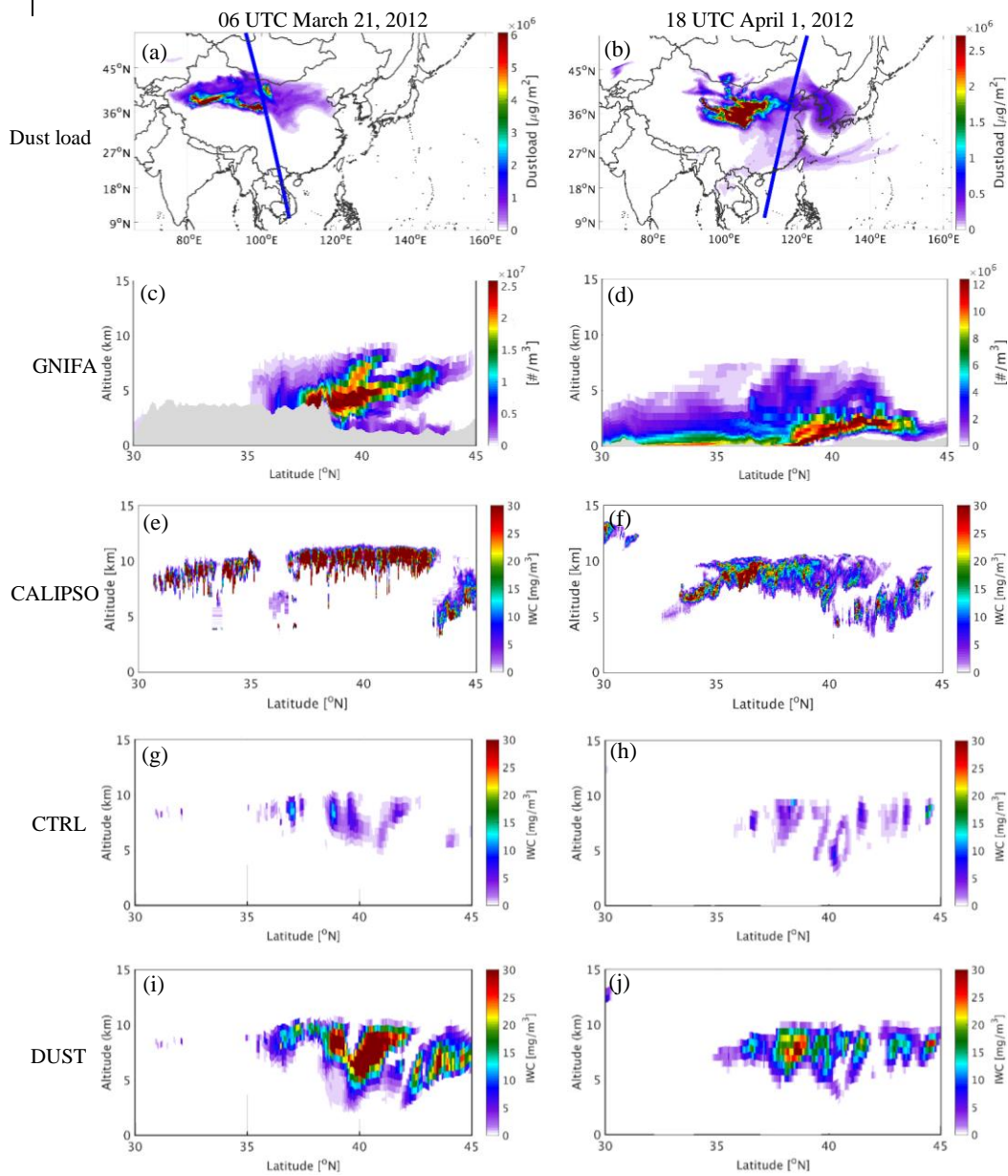


**Figure 89:** Spatial distribution for simulated dust load and satellite scanning track (a, b); the simulated vertical profile of ice-friendly aerosol (GNIFA) number concentration (c, d), with the orography represented by the shaded area; the



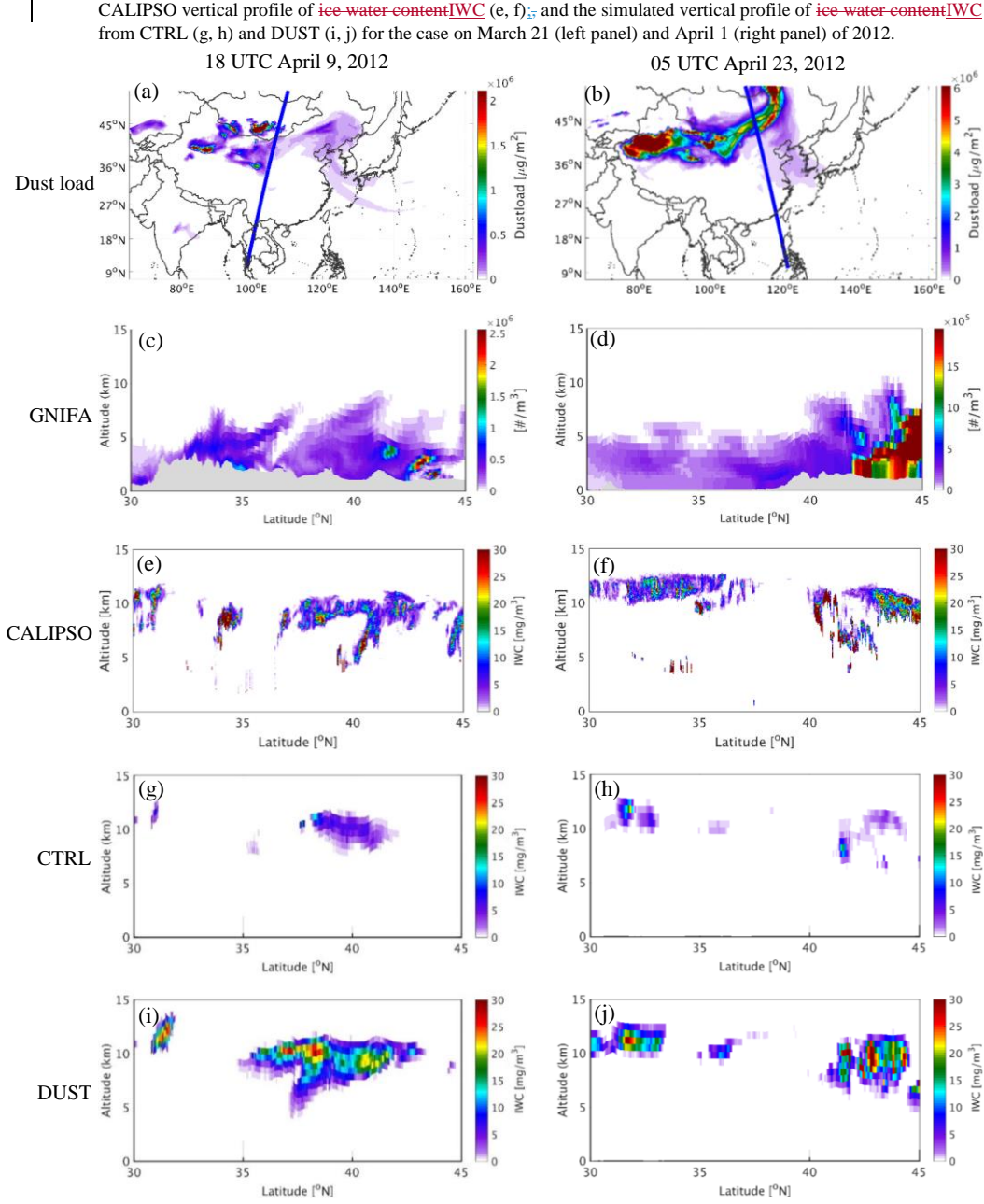


**Figure 910:** As Figure 89 but for the cases on April 9 (left panel) and April 23, (right panel) of 2012.

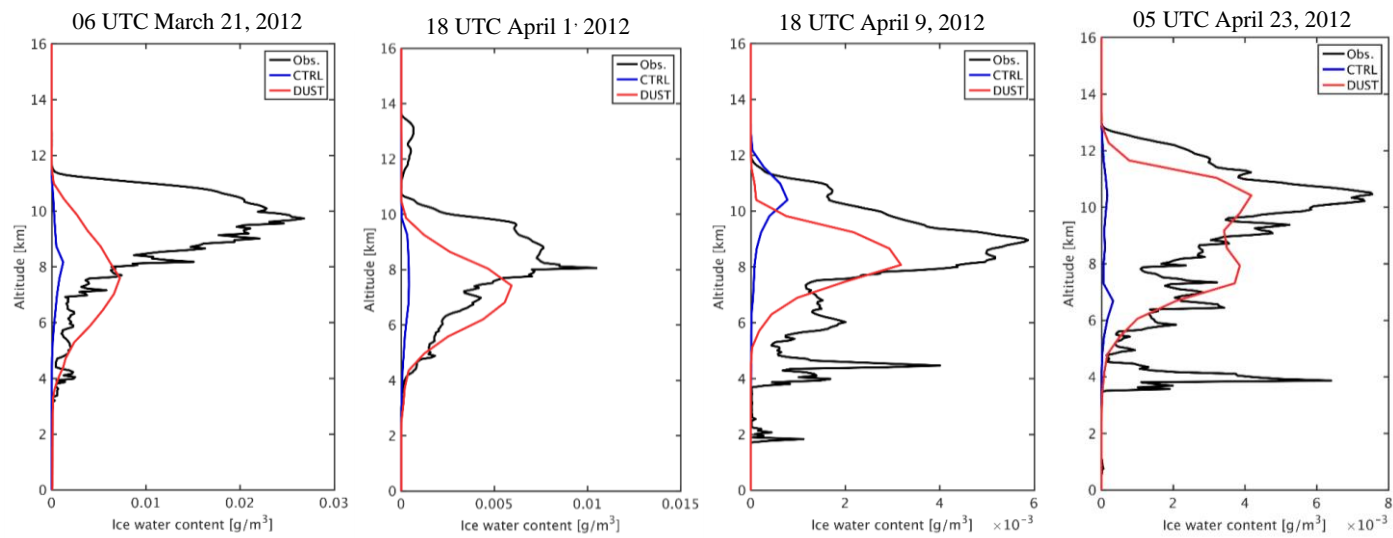


**Figure 101:** Vertical profiles for the mean observed ice water content[WC] from CALIPSO, and the simulated ice water content[WC] from CTRL and DUST for dust events on March 21, April 1, April 9, and April 23, 2012.



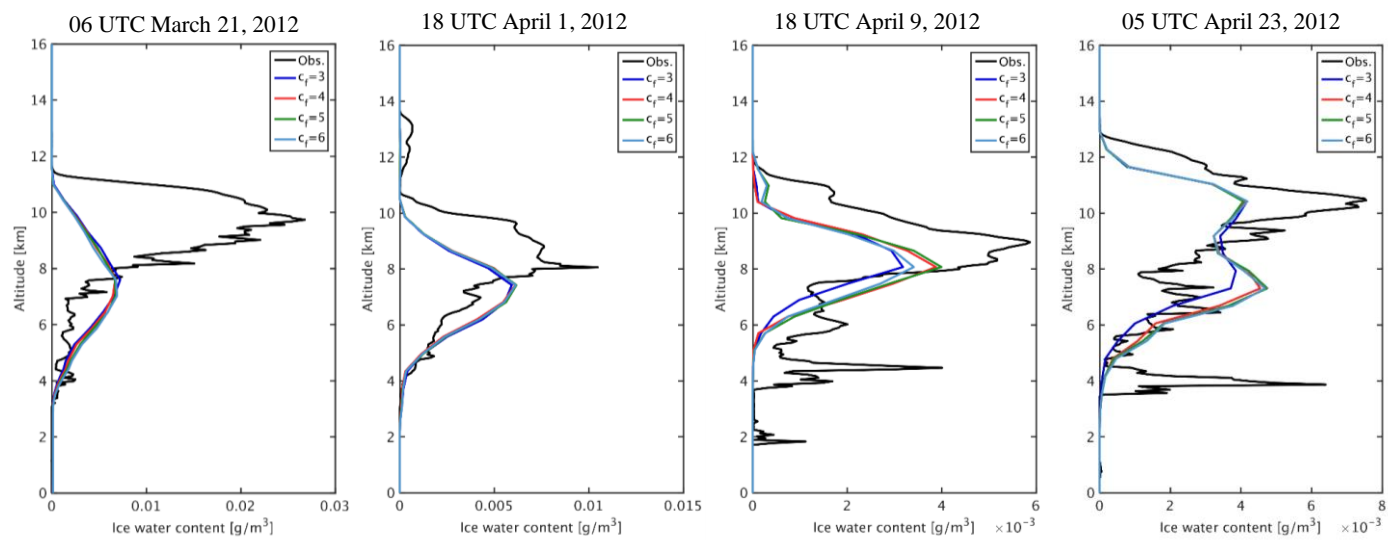


**Figure 112:** Vertical profiles for the mean observed ~~ice water content~~ IWC from CALIPSO, and the simulated ~~ice water content~~ IWC with various  $c_f$  for the dust events on March 21, April 1, April 9, and April 23, 2012.

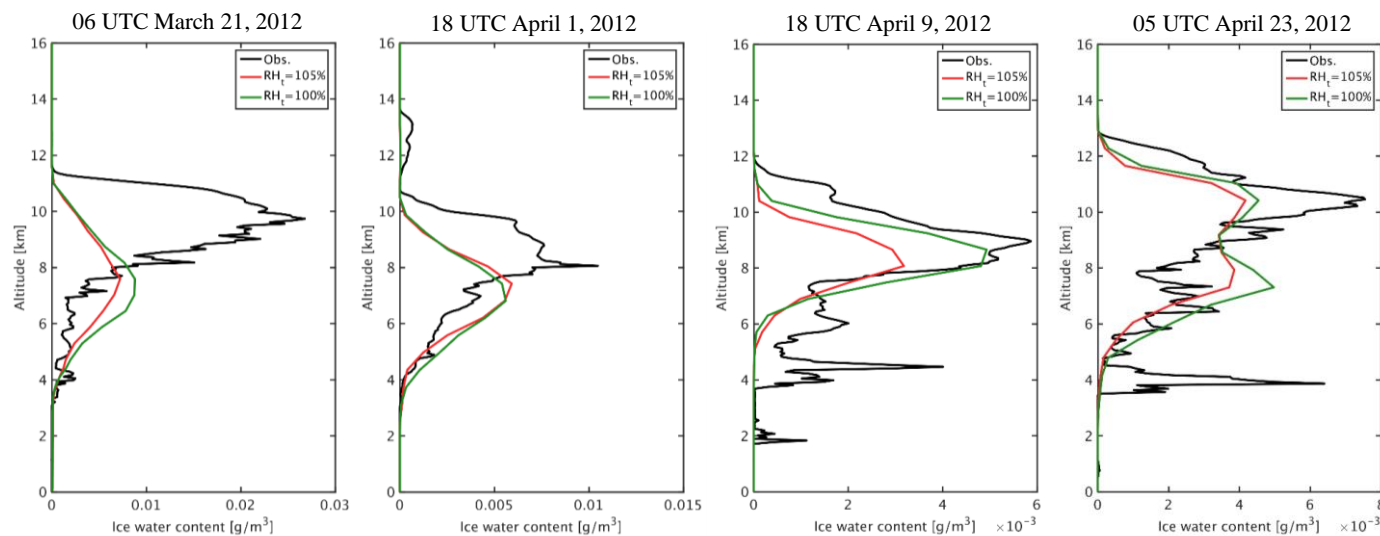


**Figure 123:** Vertical profiles for the mean observational ice water content IWC from CALIPSO, and the simulated ice water content IWC with threshold RH values of 105% and 100% for the dust events on March 21, April 1, April 9, and April 23, 2012.